FIBRA

Fostering the implementation of fibre-reinforced asphalt mixtures by ensuring its safe, optimized and cost-efficient use

Deliverable 4.1

February 2021

Braunschweig University of Technology

Braunschweig Pavement Engineering Centre (ISBS)

Universidad de Cantabria

Construction Technology Research Group

CEDR Call 2017: New Materials

Project Nr. 867481

Project acronym: FIBRA

Project title:

Fostering the implementation of fibre-reinforced asphalt mixtures by ensuring its safe, optimized and cost-efficient use

Deliverable 4.1 – Practical instructions for the design and characterization of FRAM

Submission date: 15.02.2021

Start date of project: 02.07.2018 End date of project: 30.06.2021

Author(s) this deliverable:

Chiara Riccardi, Technische Universität Braunschweig, ISBS Institut für Straßenwesen, Germany (Chapter 1, 2, 3, 4, 5)

Di Wang, Technische Universität Braunschweig, ISBS Institut für Straßenwesen, Germany

(Chapter 1, 2, 3, 4, 5)

Carlos Slebi-Acevedo, Universidad de Cantabria, GITECO (Chapter 2,3,4,5,6)

Pedro Lastra-González, Universidad de Cantabria, GITECO (Chapter 2,3,4,5,6)

Irune Indacoechea Vega, Universidad de Cantabria, GITECO (review)

Daniel Castro-Fresno, Universidad de Cantabria, GITECO (review)

Version: 01

Executive summary

This report presents the experimental results obtained from WP4 of the FIBRA project. The work consists of three parts: first, the design and mechanical characterization of different types of asphalt mixtures for surface, binder and base layers with and without fibres were evaluated; then, the potential recyclability of the Fibre Reinforced Asphalt Mixtures (FRAM) were studied; and, finally the effect of high RAP content in FRAM mixture were assessed.

This deliverable D4.1 give practical instructions about the potential application of FRAM.

The deliverable is divided into five chapters:

- CHAPTER1 consists of the motivation and introduction to the framework of the study;
- CHAPTER 2 explains the procedure to manufacture the different asphalt mixtures with and without fibres for the different layers of asphalt pavements;
- CHAPTER 3 explains the testing plan for the entire set of asphalt mixtures;
- CHAPTER 4 discusses and analyses the experimental results, underlining the effect of the fibres on the performance of asphalt mixtures;
- CHAPTER 5 highlighted the most relevant conclusions and recommendations.

Table of content

List of Tables

List of Figures

1 Introduction

Bituminous mixtures have always been valued as the most relevant material for the construction of pavement infrastructures such as motorways, highways, streets, cycle paths, and parking lots, among others. The components that constitute this composite are mainly bitumen and mineral aggregates. Nevertheless, the higher demands in the automotive fleet and the constant climate change generated by the global warming have led to the development of modified mixtures with novel additives, with enhanced characteristics that guarantee an appropriate mechanical performance to extend the long service life.

The incorporation of fibres appears as an attractive solution to extend the resilience and durability of bituminous mixtures. According to a literature review carried out in work package two, it was observed that many types of fibres had been previously investigated in bituminous mixtures, especially in dense-graded asphalt mixtures. In general, it has been observed that fibres inclusion contributes to supporting the tensile stresses transmitted to the mix by the action of traffic loads. In the same way, many improvements in the mechanical performance of the mixture, such as rutting resistance, moisture susceptibility, fatigue cracking, and dynamic modulus, have been reported. As many fibres have been widely analyzed, a novel multi-criteria analysis based on quantitative performance assessments and qualitative human judgments were implemented to do a proper evaluation and selection of the most promising fibre. Similarly, a cost-benefit, as well as an environmental impact assessment, was carried out for further analysis in the selection process. In the WP3, a preliminary study was performed to evaluate the suitable type of fibre for the conventional asphalt concrete (AC) mixture and porous asphalt (PA) mixtures. From the results, the better mechanical performance of the AC mixtures reinforced with fibres was achieved by the addition of polyacrylonitrile fibres (type P). In contrast, In the case of fibre-reinforced porous asphalt mixtures, the best results were provided by the incorporation of the set of polyolefin-aramid fibres (type A).

In this deliverable, a more detailed study was done to study the reinforcing effect of fibres in the AC and PA mixes. At the surface layer scale, the type A fibres were employed to analyze the reinforcing impact on the PA mix. Five different PA mixtures with/without fibres were prepared for comparison purposes. Air voids, Cantabro test, ITS, and moisture sensitivity were the chiefly tests taken into consideration. Concerning the AC mixtures, the 4 mm long type P fibres were taken into consideration. Different sets of AC mixtures with/without fibres were manufactured and studied in the distinct layers of the pavement structure. In addition, the potential recyclability of FRAMs was studied manufacturing artificially aged fibre-reinforced RAP (PANRAP). Finally, the feasibility of incorporating RAP without the presence of rejuvenators in the surface and binder layer was investigated. Volumetric properties, ITS, moisture sensitivity, rutting, stiffness, fatigue resistance, thermal cracking, and fracture energy were the main tests considered for comparison purposes. In the subsequent chapters, more information concerning the materials, experimental work, the discussion of results, and the most relevant conclusions are presented.

2 Materials preparation

In this chapter, the preparation procedure of the asphalt mixtures for different layers with and without fibres are presented. The asphalt mixtures were designed based on the blending procedure defined in WP3. The laboratory protocol for the production of FRAMs is shown in annex A.

2.1 Types of fibres

Two different kinds of fibres (see Figure 1) were used in this study. Type A, which consists of a combination of aramid (A1) and polyolefins (A2) fibres of 19 mm length, were used to produce porous asphalt mixtures for surface layers. The ratio of this blend of fibres is 1:7 (aramid: polyolefins). The other type that consists in polyacrylonitrile fibres (type P) of 4 mm length and nominal diameter ca. 10 um were used to produce conventional asphalt mixtures for surface, binder, and base layers. More properties' information, such as the thermal and chemical properties, of these two fibres can be found in the previous deliverable D3.2.

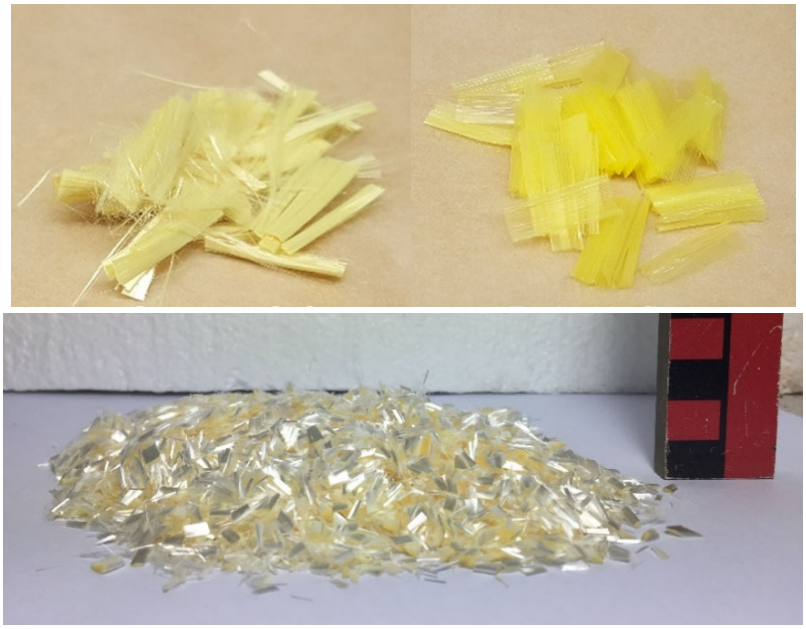

Figure 1. Different fibres used: Type A (A1: up-left, A2: up-right) and Type P (down).

During the course of this research, a provider of aramid fibres (Teijin Co.) contacted the authors of this report to propose a new type of fibres, 100% aramid, not being tested before in asphalt mixtures. The performance of these fibres was evaluated by the University of Cantabria in a different project, Safer-up (MSCA). The FRPA mixes produced with these fibres were designed with the same materials and particle size distribution in order to compare the results of both projects. A brief summary of the results are shown in annex B.

2.2 Preparation of PA and AC mixtures for surface layers with and without fibres

2.2.1 Porous asphalt (PA) mixture for surface layer

As part of the experimental plan designed in the WP4.1, a total of five porous asphalt (PA) mixes were designed and manufactured to be employed as wearing course according to the Spanish standards to evaluate their mechanical and functional performance. Table 1 illustrates the five distinct PA mixes: three of them were deemed as reference mixture while the remaining two employed fibres type A as reinforcement.

Table 1. Porous asphalt mixtures prepared for the WP4

PA16	Ref 1	Ref 2	Ref 3	FRPA 1	FRPA 2
Bitumen / mixture (%)	4.5	4.5	5	4.5	5
Type of bitumen	50/70	PMB	50/70	50/70	50/70
Type of fibre	-	-	Cellulose	Type A	Type A
Fibre / mixture (%)	-	-	0.5	0.05	0.05

All the mixes have a nominal maximum aggregate size of 16 mm, which is appropriate to be used as a surface layer. For the reference mixtures, two types of binders were employed (i.e., 50/70 penetration grade binder and PMB 45/80-65), and the optimum binder content was fixed in 4.50% by weight of the mixture. Also, a third reference mixture was designed, adding cellulose fibres and increasing the binder content to 5.0% since cellulose fibres, given their large specific surface, allow the retention of higher amounts of asphalt binder. Regarding experimental mixes, two different fibre-reinforced porous asphalt (FRPA) mixtures were manufactured with fibres type A. It is worth to mention that type A fibre was selected to be employed in PA due to the good results found in the WP3.

In all the designs, ophite was used as coarse aggregate, whereas limestone was utilized as the fine and filler fractions. For the preparation of the designs, compacted PA cylindrical specimens were manufactured following the Spanish specifications. The open-gradation curve was kept invariable (see Figure 2), which falls between the upper and lower limits of the Spanish standards.

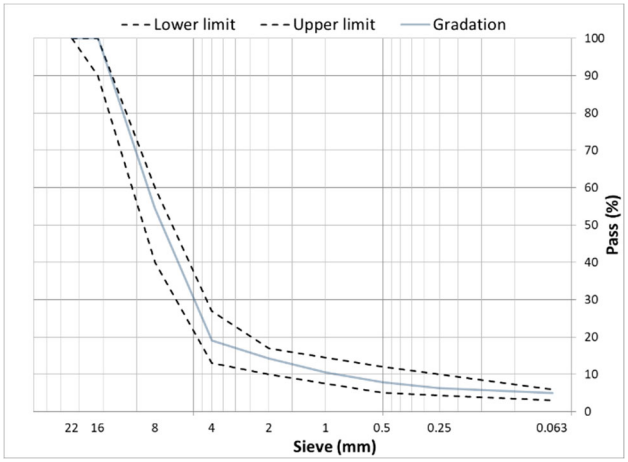

Figure 2. The particle size distribution of the PA mixes.

For the mixes prepared with a conventional binder, the mixing temperature was 150°C while in the case of the mixture done with PMB, a blending temperature of 170°C was employed according to the recommendations of the supplier. In any case, the aggregate temperatures were 15°C greater than the mixing temperature according to the bitumen type. In the case of mixtures modified with fibres, the fibre addition was done by dry method. In other words, fibres were blended with the aggregates homogeneously prior to the addition of the binder to the mix. The compaction of the specimens was done by applying 50 impacts per face with the use of a Marshall Hammer according to the European Standard EN 12697 – 30.

2.2.2 Asphalt concrete (AC) mixture for the surface layer

Regarding asphalt concrete (AC) mixes, three different AC designs were proposed to evaluate their mechanical performance. Initially, a control AC mixture was designed following the Spanish specifications with an optimum binder content of 4.30% by weight of the mix and with a voids content of 5.10%, which is an appropriate value to be used as a wearing course. Subsequently, two additional fibre-reinforced asphalt concrete (FRAC) mixtures were proposed, as can be seen in Table 2. The fibre content added to the FRAC mixtures were 0.15% of fibres type P. In the case of FRAC 1, the binder content remained constant to analyze the reinforcing effect of the fibre. In the case of FRAC 2, the binder content was increased to 4.60%, given the rate of absorption that the fibres could present.

Table 2. Asphalt concrete mixtures prepared for the WP4

AC 16	Ref	FRAC 1	FRAC 2
Bitumen / mixture (%)	4.3	4.3	4.6
Type of bitumen	50/70	50/70	50/70
Type of fibre	-	Type P	Type P
Fibre / mixture (%)	-	0.15	0.15

Similar to PA mixtures, the mixing temperature was set at 150°C as the AC designs were manufactured with a 50/70 penetration grade binder. In the same way, the fibre addition was done by the dry method, and the aggregates were preheated to a temperature 15°C higher than the final mixing temperature. Similarly, ophite was used as coarse aggregates, whereas limestone was employed as fine aggregate and filler. The particle size distribution for the three designs corresponds to an AC mixture with a nominal maximum aggregate size of 16 commonly used as a surface layer in Spain (Figure 3).

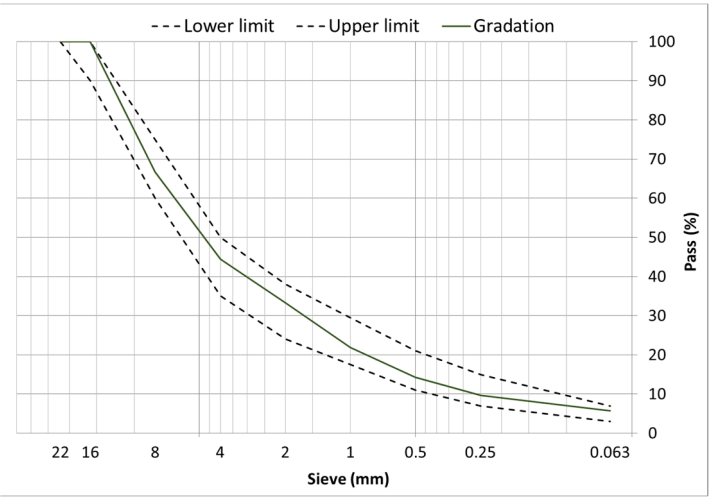

Figure 3. The particle size distribution of the AC mixes

2.3 Preparation of AC mixtures for binder and base layers with and without fibres

In accordance to the experimental plan defined in WP 4, to evaluate the performance of FRAM in the binder and base layers of an asphalt pavement, four conventional AC mixtures were designed and their mechanical properties evaluated. Table 3 summarized the materials used for the four AC mixes: two for the binder layer and two for the base layer. In particular, for the binder layer, a control mixture with polymer-modified bitumen PmB 45/80-65, and a FRAC mixture with fresh bitumen 50/70 and Type P fibre were proposed.

For the base layer, a control mixture with fresh bitumen 50/70 and one FRAC composed of fresh bitumen 35/50 and fibre type P were formulated. For all the fibre reinforced mixtures, the content of the fibre equals to 0.15% by weight of the entire mixture, as suggested by the manufactures.

Table 3. Asphalt mixtures prepared for the WP4.

Mixture	Bitumen	Fibre
Binder layer	PmB 45/80-65	-
	50/70	Type P
Base layer	50/70	-
	35/50	Type P

The following protocol was used to prepare the mixtures: the aggregates and fillers are heated up to 160°C for 10 hours, while the 50/70 and the 45/80-65 bitumens are heated up to 150°C and the 35/50 bitumen to 175°C for 3.5 hours. Before mixing, also the mixer drum is preheated at 160°C. Following the guidance of the fibres producers, the dry process was used to prepare the FRAMs, which means that no previous modification of the bitumen is done because the content of the fibres is directly added to the aggregate fraction. First, the aggregates, the filler and the fibres are mixed in the drum for 1 minute and then the bitumen is incorporated, and all the components are mixed for 2 minutes in the drum. Finally, the mixtures are compacted using the roller sector compactors. From the compacted slabs, cylindrical and prismatic samples are cut for the different tests.

2.3.1 Asphalt mixture for the binder layer

For the binder layer a common mixture AC 22 B S type in accordance to the German standard TL Asphalt-StB (2013) was designed. This mixture is composed with Gabbro aggregates with a nominal maximum aggregate size of 22 mm, intended for binder course (B) under the highest traffic loads (S). The sieving curve, reported in Figure 4, is the same for both the reference and the FRAM mixture for the binder layer. The characteristics of the receipt of the two mixtures are summarized in Table 4 where B1 is the reference mixture and B2 is the FRAM mixture.

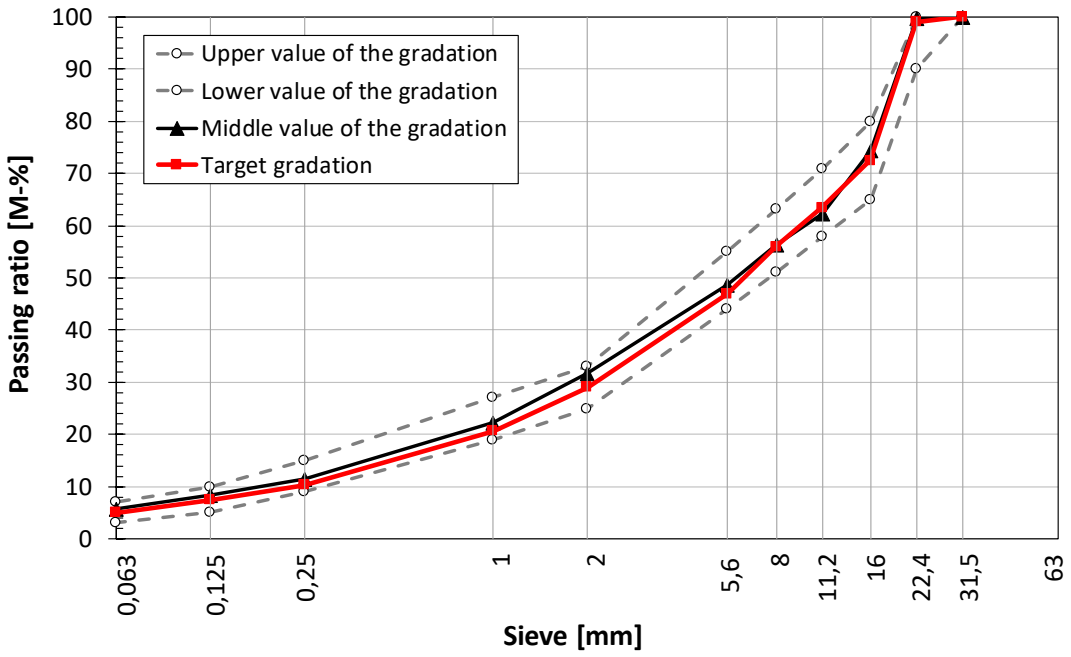

Figure 4. Grading curves for binder layer.

Table 4. Asphalt mixtures receipt for binder layer.

Fraction	B1	B2
	M [%]	
Gabbro 16/22	32	
Gabbro 11/16	7	
Gabbro 8/11	6	
Gabbro 5/8	7.5	
Gabbro 2/5	15	
Gabbro 0/2	32.5	
Sum	100	
Binder content [%]	4.4	4.4
Binder type	PMB	50/70
Fibre content [%]	-	0.15
Void content [%]	6.5	6.0
Density [g/cm^3]	2.690	2.655

2.3.2 Asphalt mixture for the base layer

For the base layer, a common mixture AC 22 T S type in accordance to the German standard TL Asphalt-StB (2013) was designed. This mixture is composed with Gabbro aggregates with a nominal maximum aggregate size of 22 mm, intended for base course (T) under the highest traffic loads (S). The sieving curve, reported in Figure 5, is the same for both the reference and the FRAM mixtures for binder layer. The characteristics of the receipt of the two mixtures are summarized in Table 5 where T1 is the reference mixture and T2 is the FRAM mixture.

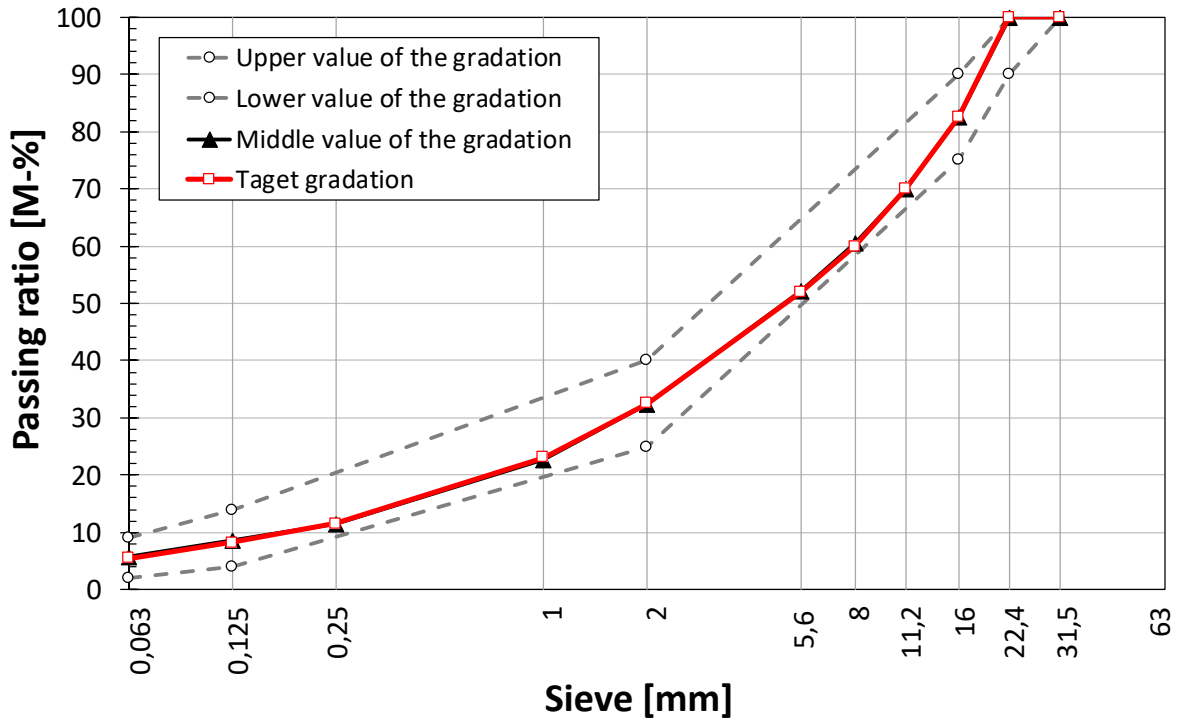

Figure 5. Grading curves for base layer.

Table 5. Asphalt mixtures receipt for base layer.

Fraction	T1	T2
	M [%]	
Gabbro 16/22	18	
Gabbro 11/16	16.5	
Gabbro 8/11	8.5	
Gabbro 5/8	6.9	
Gabbro 2/5	18.1	
Gabbro 0/2	32	
Sum	100	
Binder content [%]	4.2	4.2
Binder type	50/70	35/50
Fibre content [%]	-	0.15
Void content [%]	6.5	6.3
Density [g/cm^3]	2.689	2.636

2.4 Preparation of AC mixtures with artificially aged fibre-reinforced RAP (PANRAP)

To analyze the potential recyclability of FRAC mixtures, artificial RAP with PAN fibres (PANRAP) was prepared. To that end, a modification of the AASHTO R30 standard was proposed. According to the standard, the loose mixture is initially placed in the oven at 135°C for 4 hours to simulate the short-term oven aging (STOA). Then, the mixture is compacted and placed into an oven for 120 hours at 85°C to simulate the long-term aging performance (LTOA). Nevertheless, in this study, the LTOA procedure was also performed on the loose mixture,. The grading and the percentage of asphalt binder on the artificial RAP was the same one that was used for the production of the control mixture (FRAC 2). To evaluate the aging effect of the binder, part of the bitumen was extracted by rotary evaporator (EN 12697 – 3) and subjected to penetration (EN 1426) and softening point (EN 1427). The properties of the residual binder can be seen in Table 6.

Table 6. Characteristics of the aged binder in the PANRAP.

Characteristic	Standard	Value
Penetration at 25 °C	EN 1426	18
Softening point (°C)	EN 1427	71.4

In this research, to avoid including more control variables, no rejuvenators will be used to improve the properties of the aged bitumen within the recycled mixture. On the other hand, a softer 70/100 penetration grade binder with penetration and softening point of 73 and 48.5, respectively, was mixed with the residual aged mixture. It is expected that the softer bitumen compensates the chemical components altered by the aging process.

To prepare the AC mixtures with 50% of recycled FRAC, the following procedure was followed: 1) the PANRAP was heated in the oven at 110°C for 2 hours prior to the mixing process; 2) the remaining 50% of the new mixture was prepared by mixing the fibres with aggregates before the addition of the binder. The percentage of new fibres is the same (0.15%) but without considering the weight of PANRAP, it means the hypothesis of the residual fibres are still able to work has been considered, therefore the percentage of new fibres added to the recycled mixture is 0.075%. As said before, a softer 70/100 pen bitumen was used instead of the 50/70 pen grade used before; 3) both sets of mixtures (i.e., 50% of PANRAP and 50% of new mixture) were mixed together at 145°C until a completely homogeneous mixture was achieved. A total of two AC mixtures with artificially aged fibre-reinforced RAP were manufactured as shown in Table 7.

Table 7. AC mixture designs with PANRAP.

Mixtures ID	Natural RAP-aggregates distribution (%)		Fibre percentage contribution (%)		Type of binder used		Asphalt content (%)	
	Natural	PANRAP	New	PANRAP	Virgin	PANRAP	Virgin	PANRAP
Control-PANRAP	50	50	0	0.075	70/100	50/70	2.50	2.15
FRAC-PANRAP	50	50	0.075	0.075	70/100	50/70	2.50	2.15

2.5 Preparation of mixtures with high RAP content with and without fibres

The possibility of incorporating high percentage of RAP into FRAM is evaluated by producing and testing the following mixtures: 1) AC mixtures with 30% RAP aimed for the surface layer with and without fibres; and 2) AC mixtures with 50% RAP aimed for the binder layer with and without fibres.

2.5.1 Surface layer with 30%RAP

In this phase, two AC mixtures were designed. The first one corresponds to a control AC mixture prepared with a 50/70 pen grade binder and 30% RAP (AC – RAP), and the other one formed by 30% RAP, 0.15% of type P fibres and a 50/70 pen grade binder (FRAC – RAP). The RAP used in this phase was provided by a Spanish construction company and was obtained from a milling operation in the North of Spain. The particle size distribution of the RAP and recovered aggregates after extraction of bitumen is displayed in Figure 6.

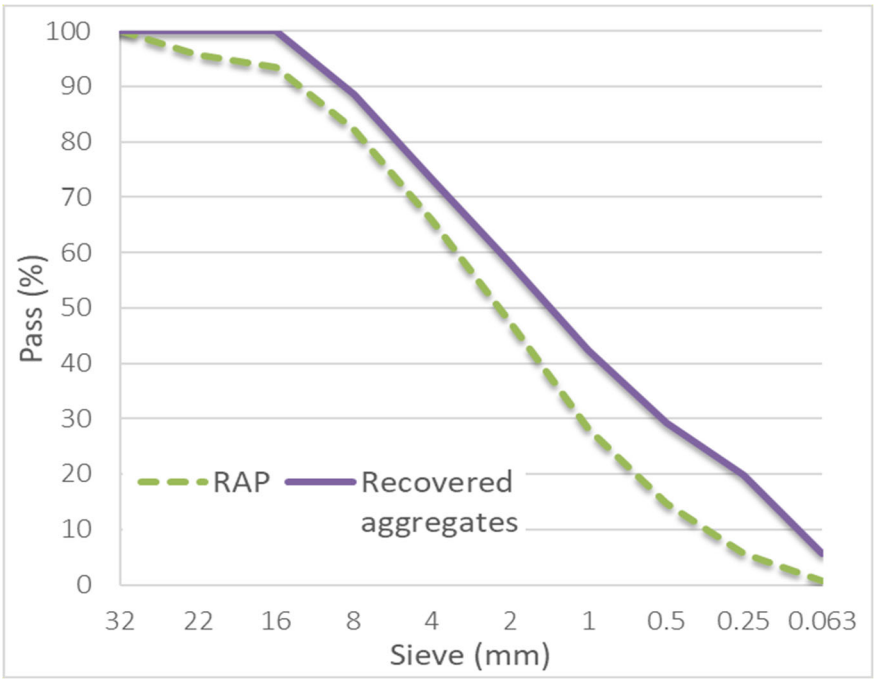

Figure 6. RAP and recovered aggregates used in the surface layer

The binder content of the RAP was determined according to EN 12697 – 1:2006, being 5.10% the percentage of recovered binder. To evaluate the properties of the residual binder, the penetration (EN 1426) and softening point (EN 1427) were calculated (Table 8). In the same way, the maximum specific gravity of the aggregates before and after the extraction of bitumen was 2.522 g/cm^3 and 2.710 g/cm^3, respectively. It worths highlighting that the different fractions of virgin aggregates and RAP were combined to achieve the final desired particle size distribution. The virgin bitumen to be added to the mixes was 3.50% by weight of the mix and was incorporated to both AC mixes. The mixing procedure was the same followed in section 2.4.

Table 8. Characteristics of the aged binder in the PANRAP.

Characteristic	Standard	Value
Penetration at 25 °C	EN 1426	6
Softening point (°C)	EN 1427	71.9

2.5.2 Binder layer with 50%RAP

Two asphalt mixtures for the binder layer were designed: one reference mixture composed of bitumen PmB 45/80-65 and 50% RAP without fibre and a mix with bitumen 50/70, 50% RAP and 0.15% of fibres. The RAP used in the present study come from a German real RAP source and its physical, geometrical and mechanical properties were evaluated. In particular, five different samples of 2500 g were sieved in accordance to EN 12697-2 and EN 13108-8 in order to obtain the black curves of the RAP. Then, on the same materials, the binder content was evaluated using the Rotatory Evaporator in accordance to EN 12697-3, 2013 and the binder was recovered. The average value of the binder content determined on 5 samples resulted 4.93%. The maximum specific gravity was also determined in accordance to EN 12697-5 and resulted 2.925 g/cm3. After the extraction, the resulting aggregates were used to evaluate the white curve in accordance to EN 12697-2 and the specific gravity reported in Table 9. Both the black and white curves are reported in Figure 7.

Table 9. Density and water absorption of the RAP aggregates.

Material	ρ_{rd} [g/cm^3]	ρ_a [g/cm^3]	ρ_{ssd} [g/cm^3]	W_{A24} [%]	Porosity [%]
RAP post 10-31	2.836	2.905	2.868	0.8	2.41
RAP post 0.063-10	2.842	2.901	2.865	0.8	2.08

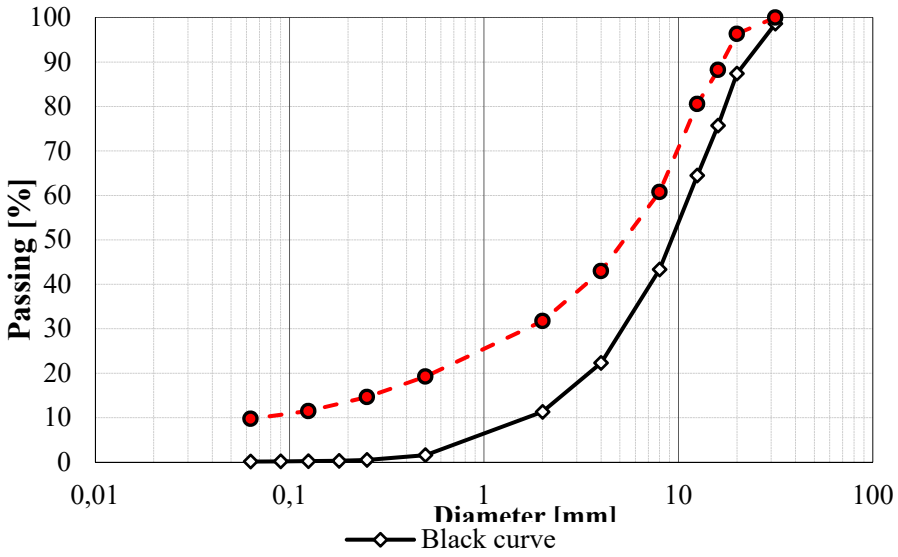

Figure 7. Black and White curves RAP source.

Based on the described properties of the RAP source, the mixture receipts reported in Table 10 were developed, where B4 is the reference mixture without fibres and B5 is the mixture with fibres. The same gradation curve reported in Figure 4 was used for both B4 and B5.

Table 10. Receipts for RAP mixtures.

Fraction	B4	B5
	M [%]	
Gabbro 16/22	21	
Gabbro 11/16	-	
Gabbro 8/11	-	
Gabbro 5/8	4	
Gabbro 2/5	10	
Gabbro 0/2	15	
RAP aggregate	50	
Sum	100	
Binder content [%]	4.4	4.4
RAP binder	2.1	2.1
Fresh binder	2.3	2.3
Fibre content [%]	-	0.15
Void content [%]	5.2	4.3
Density [g/cm^3]	2.665	2.654

3 Mechanical performance tests

In the following paragraphs, the different tests, carried out in order to characterize the mechanical properties of asphalt mixtures, are described in details.

3.1 Testing for the PA mixture for surface layers

3.2.1 Volumetric properties

Mixture volumetric properties were focused on the macroscopic evaluation, including bulk density (EN 12697 – 6) of the compacted mixture and the total air voids (T_{AV}) (EN 12697 – 8). The latter, calculated through the following equation.

$$T_{AV}(\%) = (1 - \frac{M_{dry}}{V \cdot G_{mm}}) \times 100 \quad (12)$$

3.2.4 Binder drain down

The stability of the porous mixes were also checked through the binder drain down test following the EN 12697 – 18. The mesh basket method was chosen for that purpose. The binder drainage is expressed as the percentage of bitumen draindown from the mass of the uncompacted mixture after 3 hours, according to the next equation:

$$Binder\ \ drainage\ \ (\%) = \frac{b}{m} \quad (13)$$

3.2.2 Water sensitivity test

To evaluate the sensitivity characteristics of the PA mixtures to water damage, the indirect tensile test and moisture susceptibility test was performed following the European standards EN 12697 – 23 and EN 12697 – 12, respectively. First, the indirect tensile strength (ITS) was measured in both dry and wet conditions (ITS_{dry} and ITS_{wet}) by loading the specimens diametrically across the circular cross-section at a constant rate of 50 mm/min and measuring the peak strength to the failure. For wet conditioning the mixtures, the samples were immersed in a water bath at 40°C for 72 hours before carrying out the test. The moisture susceptibility is assessed by calculating the indirect tensile strength ratio (ITSR) using the following formula.

$$ITSR = \frac{ITS_{wet}}{ITS_{dry}} \times 100\% \quad (14)$$

3.2.3 Particle loss

Cantabro loss particle test (EN 12697 – 17) was carried out to assess the raveling potential of the PA mixes. This test measures the percentage of particle loss that occurs when the specimen is subjected to abrasion in the Los Angeles machine. The Cantabro test was also performed in wet conditions according to the NLT 362/92 Spanish standard. In this case, the specimens were immersed in water at 60 °C for 24 hours. Then the samples were kept at 25°C

for another 24 hours before performing the test. In both cases, the loss in mass after 300 turns in the Los Angeles machine is expressed in percentage and is calculated according to Equation 14.

$$Particle\ loss(\%) = \frac{m_i - m_f}{m_i} \times 100 \quad (14)$$

Where m_i and m_f correspond to the initial and final mass of the specimens.

3.2 Testing for the AC mixtures for surface, binder and base layers

3.2.1 Water sensitivity test

The water sensitivity test was performed according to the European standard EN 12697-12 Method A. Hence, a set of 8 specimens (D=100 mm, h=60 mm) was divided into two equally sized subsets and conditioned. One subset was maintained dry in a climate chamber at 22 °C while the other subset was saturated and stored in water at elevated conditioning temperature (40°C) for 68 to 72h. After conditioning, the indirect tensile strength of each of the two subsets was determined in accordance with EN 12697-23 at the specified test temperature of 22°C (Equation 1). The ratio of the indirect tensile strength of the water conditioned subset compared to that of the dry subset is determined in accordance with Equation 2 and expressed in percentage (%). The parameter of ITSR was applied to evaluate the effect of fibres.

$$ITS = \frac{2F}{\pi Dh} \quad (1)$$

$$ITSR = 100 \cdot \frac{ITS_w}{ITS_d} \quad (2)$$

where,

ITS indirect tensile strength (MPa);

F force (N);

D and *h* diameter and the height in mm, respectively;

ITSR the indirect tensile strength ratio, in percent (%);

ITS_w the average indirect tensile strength of the wet group in;

ITS_d the average indirect tensile strength of the dry group.

3.2.2 Stiffness

For determining the stiffness modulus of the asphalt mixtures, Direct tension-compression tests in accordance with EN 12697-26, Annex D were performed on three replicates for each type of mixtures. According to the specification, a sinusoidal load is introduced into a cylindrical sample (50 mm x 160 mm) glued on two steel plates screwed to the loading rig. The stiffness tests were carried out at different temperatures (-20, -10, 0, 10, 20 and 30°C) and at several frequencies 0,1; 0,3; 1; 3; 5 and 10 Hz. In order to assure to be in the linear range a stress amplitude of 0.10 MPa was applied for temperature from -20°C to 10°C and 0.05 MPa was

applied for 20 and 30°C.

The results are the stiffness modulus and the phase angle versus frequency and temperature. The master curves of the complex modulus and of the phase angle were plotted using the model described in NCHRP 459 and reported in Equations 3 and 4 together with the William-Landeln- Ferry (WLF) equation (Equation 5) for the calculation of the shift factors.

$$E^* = E_e^* + \frac{E_g^* - E_e^*}{\left[1+\left(f_c/f'\right)^k\right]^{m_e/k}} \quad (3)$$

$$\delta = 90 - (90 - \delta_m)\left\{1+\left[\frac{\log(f_c/f')}{R_d}\right]^2\right\}^{-m_d/2} \quad (4)$$

where,

$E_e^* = E^*(f \to 0)$ the equilibrium complex modulus;

$E_g^* = E^*(f \to \infty)$ the glass transition complex modulus;

k, m_e, R_d and m_d dimensionless shape parameters;

f_c the location parameter with dimensions of frequency, E_g^* and me asymptotes intercept;

$f_c' = f_c\left(\frac{E_e^*}{E_g^*}\right)^{1/me}$ the frequency where the E_e^* and m_e asymptotes intercept;

f' the reduced frequency, function of both temperature and strain;

δ the phase angle;

δ_m the maximum value of the phase angle;

f_d the location parameter at which δ_m occur.

$$\log a_t(T) = -\frac{c_1(T - T_0)}{c_2 + (T - T_0)} \quad (5)$$

where,

a_t the time-temperature shift factors;

c_1 and c_2 regression coefficients;

T_0 the reference temperature.

In the case of the AC mixtures designed for the surface layer (**section 2.2.2**), the stiffness was evaluated by means of the four-point bending test according to the European Standards EN 12697 – 26 (Annex B). The stiffness test was conducted at 20°C under strain-controlled mode with a strain amplitude of 50 μm/m. The modulus and the phase angle of different frequencies, starting from 0.1 Hz to 30 Hz were recorded directly from the testing apparatus.

3.2.3 Rutting resistance

Rutting resistance (permanent deformation) test was assessed by using the wheel tracking test device according to the European Standard EN 12697-22. The entire set of asphalt mixtures reported in Chapter 2 were tested. The testing device and the related sample are illustrated in Figure 8. In this test, the susceptibility of asphalt mixture to deform was determined observing the rut formed by repeated passes of a loaded wheel at a constant temperature of 60 ºC. The wheel tracking tests were conducted on compacted slabs (two samples for each asphalt mixture) with dimension of 500 mm × 180 mm × 100 mm. After a zero measurement the relative rut depth, e.g., the absolute rut depth as a percentage of the specimen height, was determined at different time intervals.

Figure 8. Rutting resistance test according to EN 12697-22.

3.2.4 Fatigue resistance

The fatigue resistance of the AC mixtures designed for the binder and base layers was investigated based on the European Standard EN 12697-24. Cylindrical specimens with dimension of 100 x 40 mm was used to perform the Indirect Tensile Test (IDT), subjecting them to a continuous sinusoidal load. The testing set-up is illustrated in Figure 9. The loading frequency of 10 Hz and two constant temperatures of 20 ºC and 10°C were used in this study. Through the vertical load, a state of strain is produced in the middle of the specimen that leads to its eventual failure. According to the standards, five loading amplitudes, were implemented allowing the loading cycles to reach the fatigue criterion (Equation 4). The smallest loading amplitude is chosen in that way that the specimen fails after 10^6 cycles and the largest amplitude so that the specimen withstands at least 10^3 cycles. The entire set of asphalt mixture reported in Chapter 2 was tested. 30 specimens were tested, three samples for each of the five strain levels and for each temperature.

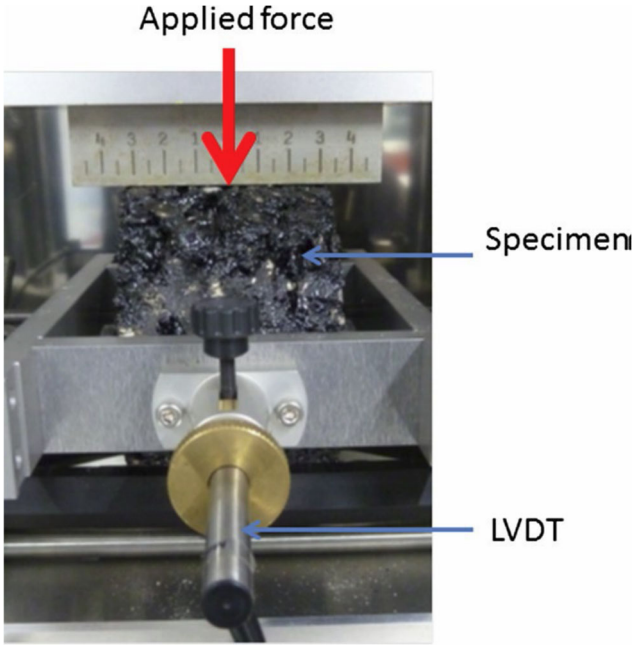

Figure 9. Test set-up for the indirect tensile test.

According to the standard, two parameters were selected to evaluate the fatigue resistance: the numbers of loading cycles, N_{macro}, when energy ratio (*ER*) (Figure 7a) reached its peak, as the product of the number of cycles and stiffness modulus (Equation 6):

$$ER(N) = \left|E(N)\right| N \tag{6}$$

where,

$E(N)$ the stiffness modulus at the particular cycle N.

Conventionally, the Wöhler line (Equation 7) can be used to express the material's fatigue function as shown in Figure 10. Five different strain amplitudes for each testing condition were selected to build this line.

$$N_{Macro} = C_1 \cdot \varepsilon_{el}^{C_2} \tag{7}$$

where,

ε_{el} horizontal elastic initial strain;

C_1, C_2 fitting constants.

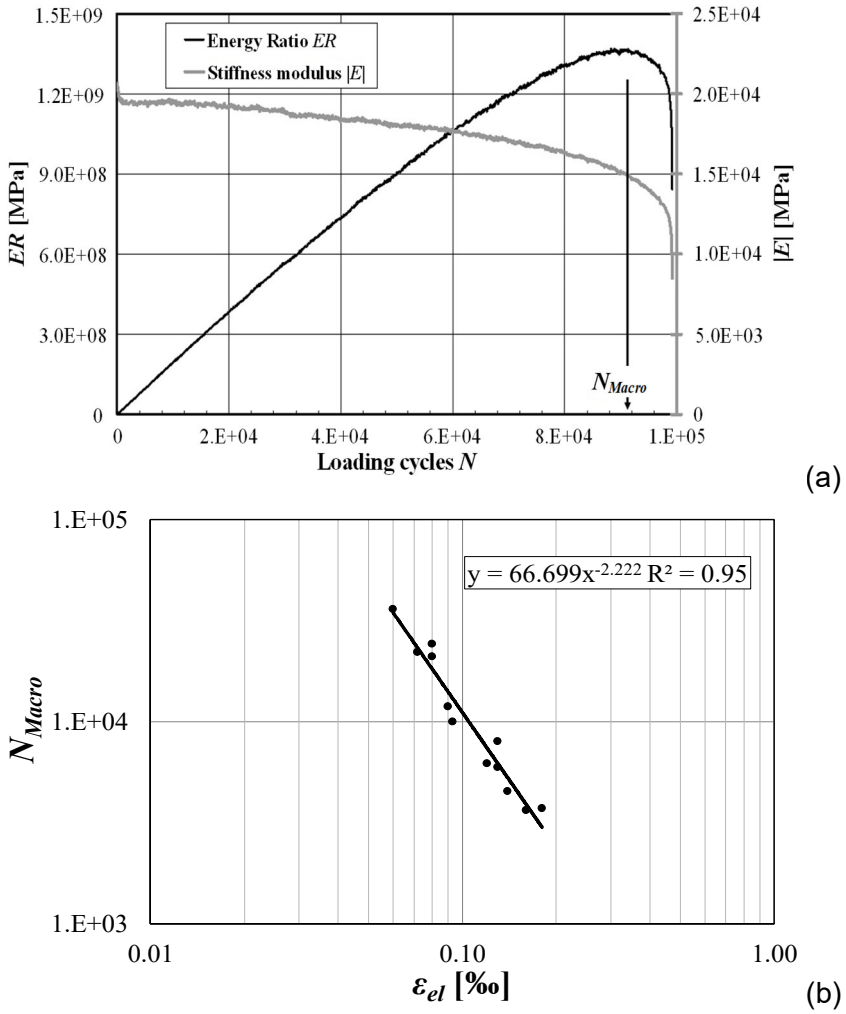

Figure 10. (a) Schematic to obtain the Nmacro based on the maximum value of ER at f=10Hz; (b) an example of fatigue function (Wöhler line) at T=20 °C and f=10 Hz.

Furthermore, from the fatigue line the classical parameter ε_6 defined as strain to reach one million cycles was also calculated.

The fatigue resistance of the AC mixtures designed for the surface layer (section 2.2.2) was tested by means of the four-point bending test according to the European Standard EN 12697 – 24 (Annex D). The testing set-up is illustrated in Figure 11. The test was conducted at 20°C, applying a frequency of 30 Hz under strain-controlled mode. The strain amplitude varied in a range from 100 to 350 µm/m. In this test, the main parameters obtained are the strain at one million cycles and the fatigue law through the following equation.

$$\ln N = c_1 - c_2 \ln \varepsilon \quad (8)$$

Where *N* is the number of loading cycles for a given level of strain ε (µm/m) ; *C1* and *C2* are the fatigue constants.

Figure 11. Test set-up for the fatigue resistance test

3.2.5 Thermal cracking resistance and fracture energy

In order to study the performance of the asphalt mixtures at low temperatures, two different types of tests were used for the entire set of asphalt mixture presented in Chapter 2: the Thermal Stress Restrained Specimen Test (TSRST) and the Semi Circular Bend (SCB) test.

The TSRST (Figure 12) were performed in accordance to EN 12697-46. Prismatic asphalt beams with dimensions of 50x50x160 mm³ were cut from the slabs. During the test, the specimen is held at constant length, while its temperature is decreased from a starting temperature of + 20 °C, with a constant cooling rate of ΔT = -10 K/h. A close-loop control system keeps specimen at constant length. Due to the prohibited thermal shrinkage, the specimen is subjected to an increasing (cryogenic) tensile stress. The test ends at a minimum test temperature of T = -40 °C or at failure, when the cryogenic stress reaches the tensile strength of the asphalt sample.

The TSRST results consist in a temperature-dependent function of cryogenic stress σ_{cry} (T) [MPa], in failure stress σ_F [MPa] and in failure temperature T_F [°C].

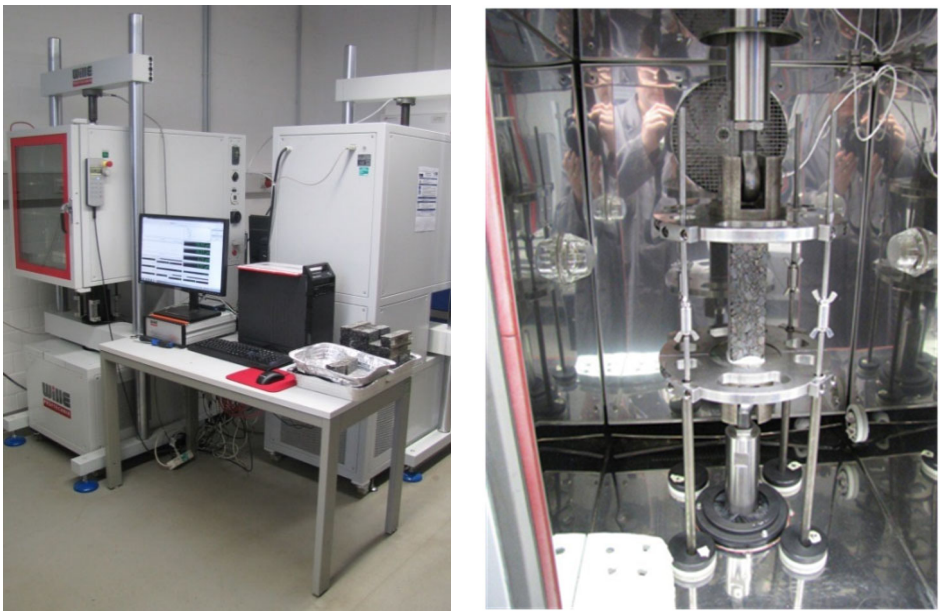

Figure 12. TSRST test device.

The SCB fracture tests were performed based on EN 12697-44. A notched semi-circular shaped specimen with a diameter of 150 mm and a thickness of 30 mm was used for this purpose. A straight vertical central notch of 15 mm (20% of the height) in length and around 1 mm width was fabricated on the plane side of the specimens with a high precision band saw to avoid potential wavy notch with an irregular shape. The sample was placed on a frame consisting of two fixed rollers and having a span of 120 mm. In order to control the strain evolution during the test, two displacement sensors were attached to the testing frame and to the specimen: a Load Line Displacement (LLD) and a Crack Mouth Opening Displacement (CMOD). The configuration is shown in Figure 13. The stable evolution of the crack opening was obtained through a closed loop system governed by the CMOD signal and a sufficiently low rate of loading rate, the loading rate needs to be adjusted for different materials and different temperatures.

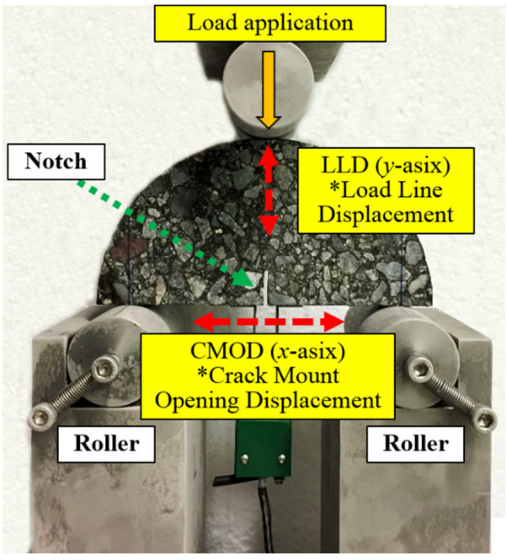

Figure 13. SCB test device.

A single testing temperature of -18 °C was selected in this project. For each material, at least two replicators were performed.

Based on the European standard 12697-44, the critical nominal stress σ_{max}, and two main fracture parameters, fracture energy, G_F, and fracture toughness K_{Ic} can be calculated:

$$G_F = W_F / A_{lig} = \int P du / A_{lig} \quad (9)$$

$$K_{Ic} = \sigma_{\max} \cdot Y_I \quad (10)$$

$$Y_I = -4.9965 + 155.58(\frac{a}{r}) - 799.94(\frac{a}{r})^2 + 2141.9(\frac{a}{r})^3 - 2709.1(\frac{a}{r})^4 + 1398.6(\frac{a}{r})^5 \quad (11)$$

Where,

W_F	work of fracture
A_{lig}	ligament area, which $A_{lig}=(r-a)\times t$
Y_I	the normalized stress intensity factor (dimensionless)
σ_{max}	$P_{max}/(2\cdot r\cdot t)$
r	radius or the height of the sample
t	thickness;

4 Experimental results and analysis

In the following chapter, the experimental results of the tests described in Chapter 3 are summarized and analysed.

4.1 Results on the PA mixtures for surface layer with and without fibres

4.1.1 Bulk density and air voids

The bulk density and the air voids of the PA mixtures are presented in Figure 14. In general, all the mixtures have a total air voids content greater than 20% with an exception of the Ref 3, which displayed an air voids content of 19.20%. Adding fibres type A did not generate significant changes in the porosity of the mixtures. The FRPA 2 design with 0.05% fibres and 5.00% of binder content slightly reduced the voids but still higher than 20%.

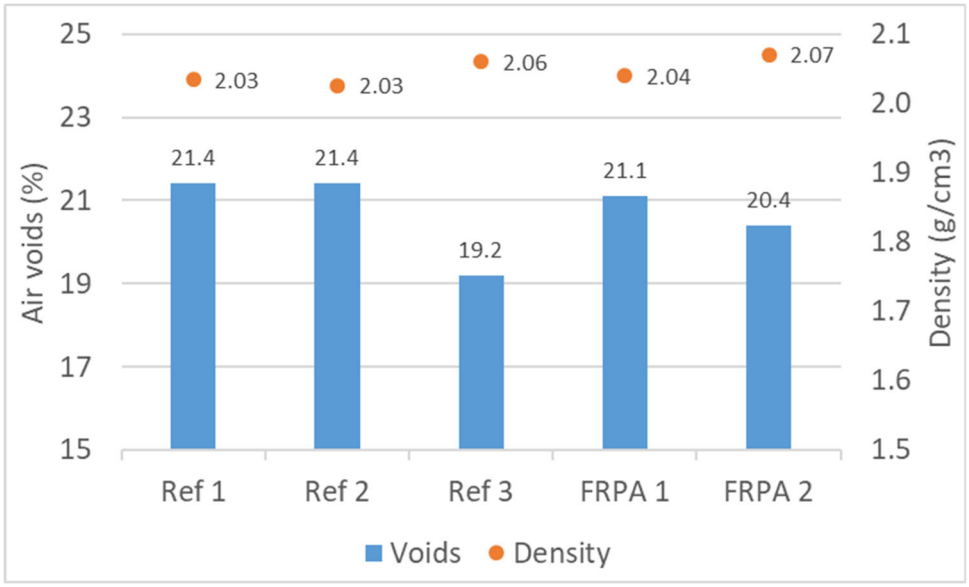

Figure 14. Density and total air voids of the PA mixtures (EN 12697 – 8)

4.1.2 Water sensitivity test

Figure 15 presents the results concerning the ITS in both dry and wet conditions as well as the ITSR measured in percentage. As can be seen, adding type A fibres leads to an increment in the ITS values in dry conditions. Better results were obtained in FRPA 2 with a higher binder content. In the same way, it is essential to mention that adding type A fibres led to a higher ITS value in dry conditions as compared to Ref 2, which was prepared with a polymer-modified binder. Regarding ITS in wet conditions, the FRPA 2 design also displayed the highest value, followed by Ref 3 and FRPA 1 mix in the lowest position. From the results, it is believed that an increase in the bitumen content is needed to properly coat the fibres.

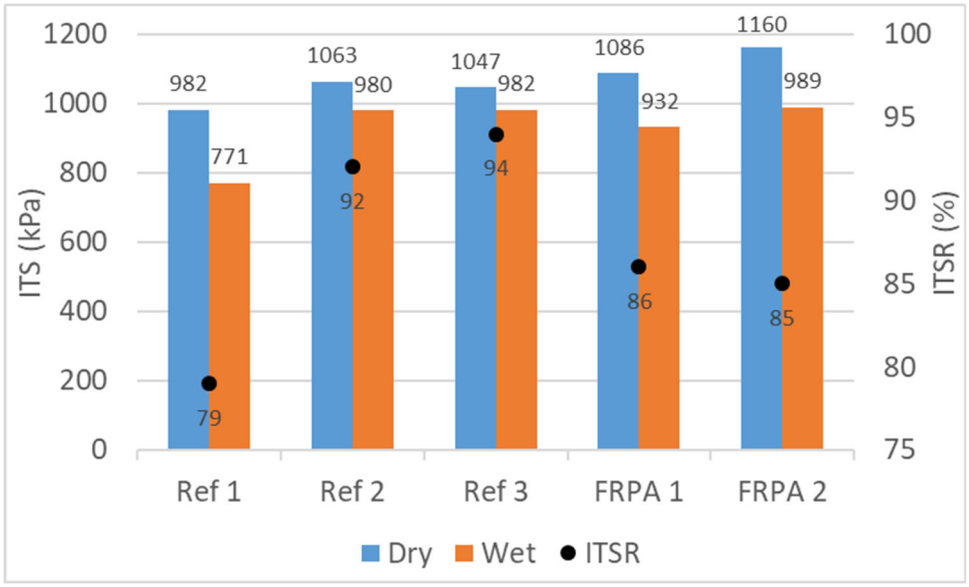

Figure 15. Indirect tensile strength and moisture sensitivity results

Concerning water sensitivity results, Ref 3 and Ref 2 depicted the highest moisture resistance capability, followed by FRPA mixes and Ref 1 with the lowest value, so both, the addition of a PMB or cellulose fibres to the PA mixture effectively reduce their sensitivity to water. The addition of type A fibres seems also to present a positive effect on this property but in a lesser extent.

4.1.3 Particle loss results

The particle loss in dry and wet conditions is displayed in Figure 16. The FRPA 2 mixture presented the highest raveling resistance in dry conditions, followed by the mixture manufactured with the polymer modified binder (Ref 2). Comparing the results with PA using plain 50/70 penetration grade binder, it can be concluded that the addition of fibres reduces the particle loss in dry conditions. Concerning the particle loss under the action of water, the best results were obtained with the use of a polymer-modified binder. On the other hand, FRPA 1 displayed the worst result, with a particle loss of 39.8%. However, increasing the binder content, the fibres are adequately coated, notably minimizing the loss of particles, although in a lesser extent than PMB(we should consider the percentage of voids of each type of mixture)s.

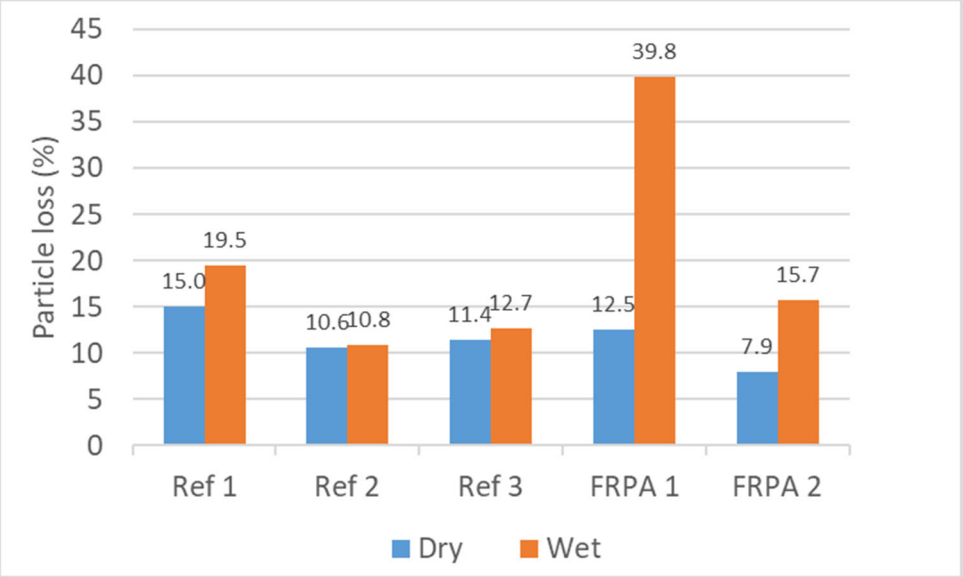

Figure 16. Particle loss results in dry and wet conditions

4.1.4 Binder drain down results (PA mixes)

Due to the low binder content, the mixtures are not prone to present binder drain down. However, to check the stabilizing potential of the fibres the binder drain down test was done and the results are presented in the Table 11. Effectively none of the mixes is prone to binder drainage. The FRPA 2 showed a minimum value of 0.03%, fulfilling the limit of 0.3% established in the scientific literature.

Table 11. Binder drain down results

PA16	Ref 1	Ref 2	Ref 3	FRPA 1	FRPA 2
Binder drain down (%)	-	-	-	-	0.03

4.1.5 Thermal cracking resistance and fracture energy

The average values of failure temperature (T_F) and failure stress (σ_F) from TSRST on three replicates for each mixture are given in Table 12. It can be easily found that the FRAM mixture has a much worse thermal cracking behaviour respect to the corresponding reference mixture. The difference between the failure temperatures of the two mixtures is almost 10 °C, while the failure stress is not so different. In this case, clearly the impact of the fibre does not reach the performance of the PMB.

Table 12. Results of the TSRST.

Mixture	Failure Temperature T_F [°C]	Failure Stress σ_F [MPa]
Ref 2	-33.9	1.455
FRPA 2	-24.2	1.114

Regarding the SCB tests, a single testing temperature of -18 °C was applied for each mixture, very good repeatability is found between each sample. In Table 13, the calculated nominal stress, σ_{max}, fracture energy, G_F, and fracture toughness, K_{IC} for are summarized. In Figure 17,

the curves of the nominal stress vs. relative CMOD for these two different PA mixtures are illustrated. In Table 13, overall higher values can be found in the materials prepared without fibre. In the case of Figure 17, an overall higher curve is found for the one without fibres. In both mixtures, curves show very similar trends after the peak, it is to say that both mixtures have similar fracture resistance response and brittleness behavior. It can be concluded that materials without fibre have slightly better fracture resistance than the one prepared with fibres.

Table 13. SCB calculated parameters for surface PA mixtures at -18 °C.

Mixtures	σ_{max} [MPa]	G_F [J/m^2]	K_{IC} [MPa*m$^{1/2}$]
Ref 2	2.461	1.040	17.855
FRPA 2	1.997	0.627	14.648

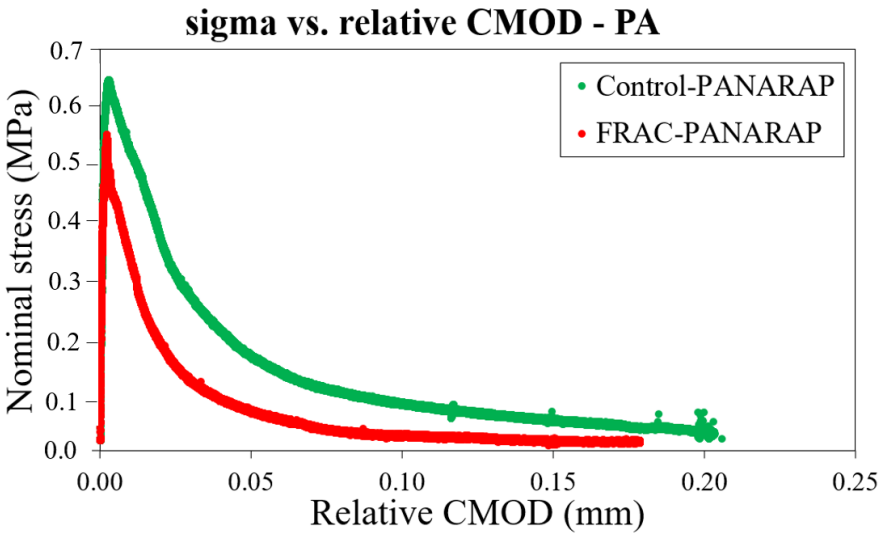

Figure 17. Comparison curves of different samples in T2.

4.2 Results on the AC mixture for surface layer with and without fibres

4.2.1 Bulk density and air voids (AC mixtures)

The results concerning the bulk density and the air voids are presented in Table 14. In the same way, the Marshall test was applied to the specimens once the volumetric properties were calculated. Accordingly, the Marshall Stability and flow values were recorded as appeared in the table. From the results, the FRAC mixtures showed a slight increase in the void content in comparison to the control AC mixture. However, not notable changes were observed in the Marshall stability as well as in the flow value.

Table 14. Bulk density and air voids of AC mixtures

Bulk density and voids EN 12697 - 8	Units	Control		FRAC1		FRAC2	
		Mean	SD	Mean	SD	Mean	SD
Density	g/cm3	2.45	0.01	2.42	0.00	2.43	0.00
Voids in mixture	(%)	5.10	0.36	6.17	0.10	5.58	0.16
Voids in aggregates	(%)	15.29	0.32	16.29	0.09	16.42	0.14
Marshall Stability	kN	15.75	0.85	16.23	0.70	15.91	0.53
Flow	mm	3.80	0.28	4.23	0.61	4.74	0.61

4.2.2 Indirect tensile strength and moisture sensitivity

Figure 18 illustrates the comparative results between dry and wet conditions of the AC mixtures as well as the ITSR value obtained from the indirect tensile test. As can be observed, the highest ITS value in dry conditions was obtained by the FRAC 2 mixture followed by the control mixture and the FRAC 1 in the last position. Similarly, the FRAC 2 mixture displayed the greatest ITS_{wet} response with an increase of 8.43% in comparison to the control mixture whereas the FRAC 1 mix displayed similar results to the control mixture. Concerning the ITSR, the three mixes showed appropriate moisture resistance capability since, in the three cases, the ITSR were higher than 85%.

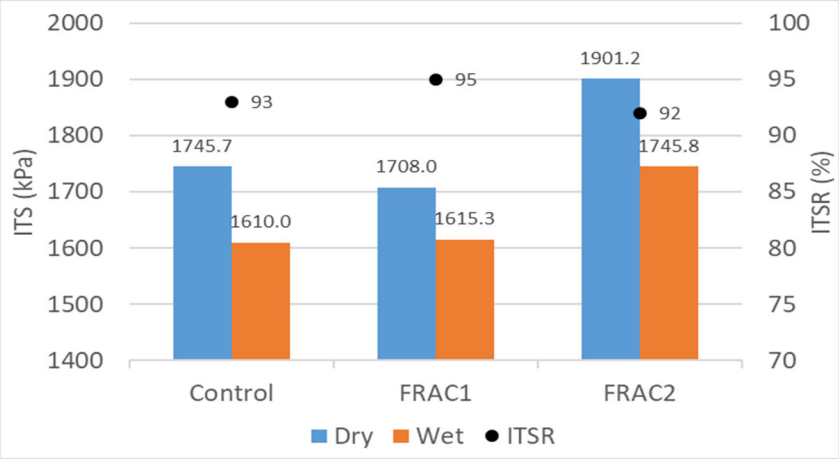

Figure 18. ITS and ITSR results for AC mixtures

4.2.3 Rutting

Table 15 displays the results obtained from the wheel tracking test. From the test, the linear slope or rate of deformation (mm/1000 cycles) was calculated per each mixture as well as the rut depth (mm) once 10.000 load cycles were applied (20.000 passing). According to the results, FRAC 1 and FRAC 2 mixtures depicted remarkable improvements in both the slope and rutting depth in comparison to the control mixture. It is worth to highlight that despite the slight increase in the binder content of FRAC2 mixture over the FRAC1 mixture, there were not notable differences in both slope and rut depth. Consequently, it verifies the fact that fibres help to stabilize the mix.

Table 15. Rutting results

Wheel tracking test EN 12697 - 22	Units	Control		FRAC1		FRAC2	
		Mean	SD	Mean	SD	Mean	SD
Slope	mm/1000 cycles	0.10	0.03	0.03	0.01	0.03	0.01
Rutting depth	mm	3.43	0.35	2.07	0.15	2.37	0.06

4.2.4 Stiffness

From the stiffness test, the dynamic modulus, as well as the phase angle, were recorded at different levels of frequencies, as shown in Figure 19. Based on the results, the FRAC1 mixture presented higher values of dynamic modulus and lower values of phase angle for all the frequencies when compared to the control mixture. The increase in modulus and the decrease in the phase angle supposes a more elastic and stiffer mixture than the control mixture. On the other hand, the FRAC2 mixture presented lower values of phase angle and greater response in the modulus. The above could be because this mixture has a higher bitumen content, making it less rigid and more viscous. However, not significant differences were observed between the mixtures.

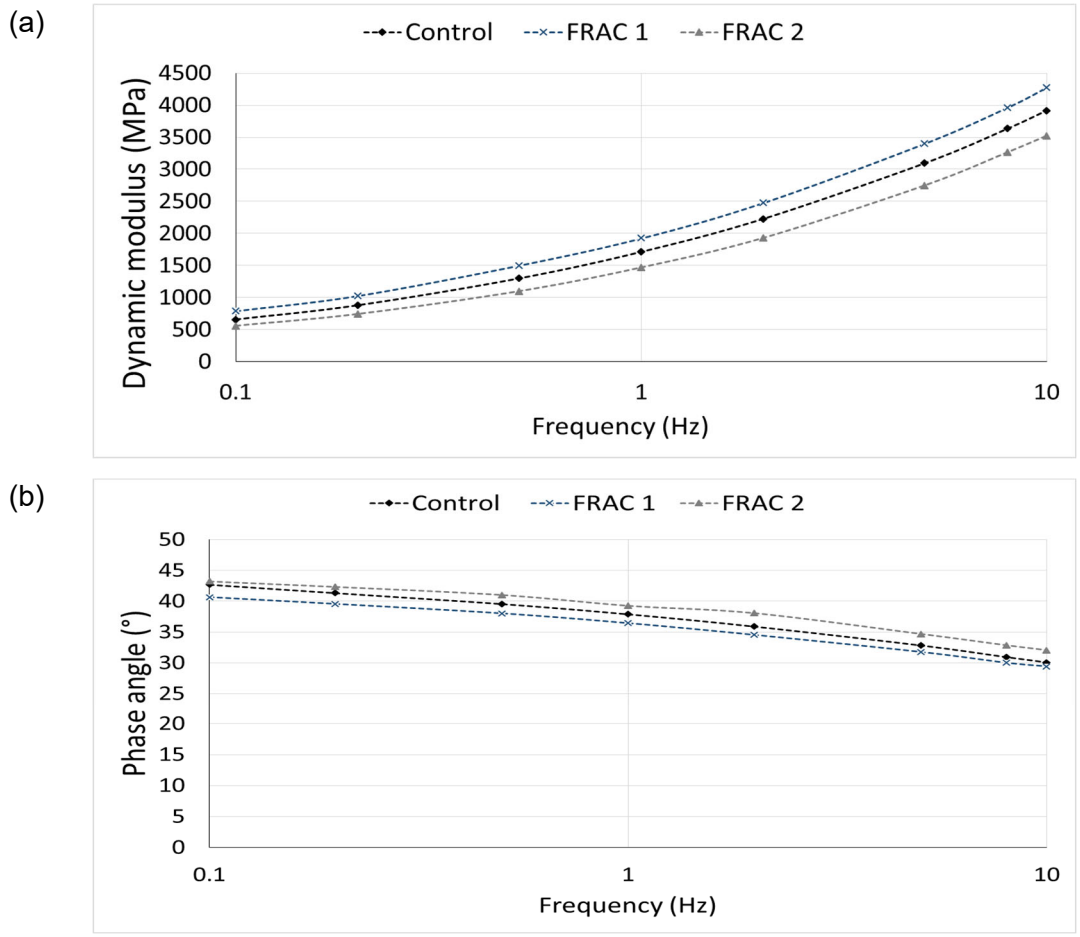

Figure 19. Results of the AC mixtures: (a) dynamic modulus; and (b) phase angle.

4.2.5 Fatigue resistance

Figure 20 displays the experimental results obtained from the fatigue test. The graph shows the number of loading cycles on the logarithm scale (x-axis) for a given level of strain on the arithmetic scale (Y-axis). The initial stiffness at 30 Hz (S_0) after 100 cycles, the characteristic strain after one million cycles, the number of cycles to failure at 100 microstrain, the constants of the fatigue law, and the R^2 values can be seen in Table 16. The effect of the type P fibre in FRAC 1 and FRAC 2 is different. While FRAC 1 (with the same percentage of bitumen of the reference) presents a higher stiffness maintaining practically the same fatigue resistance, the FRAC 2 (with a higher percentage of bitumen) shows a reduction in the stiffness but with a significant increase of its resistance against fatigue.

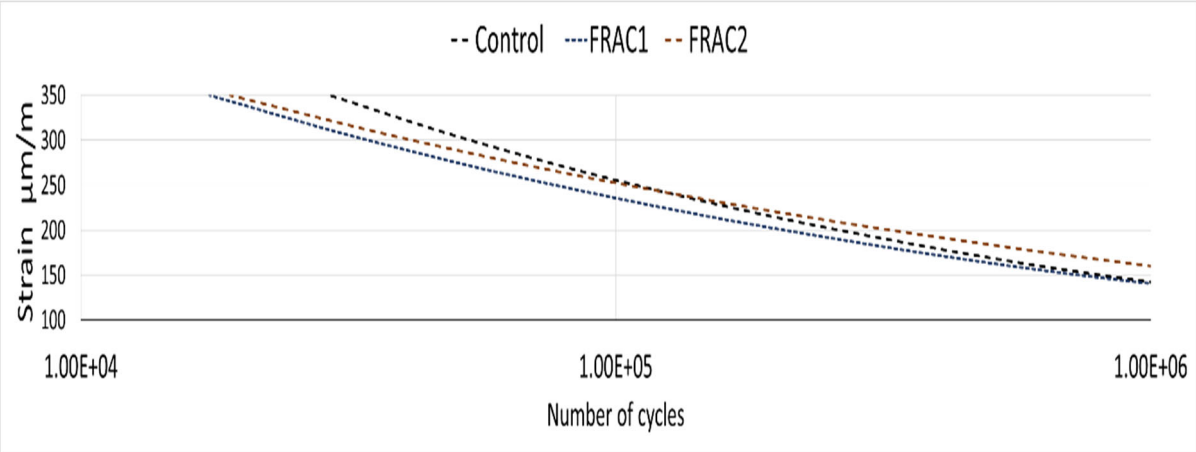

Figure 20. Fatigue testing results

Table 16. Main parameters obtained from the fatigue resistance test

Parameter	Unit	Control	FRAC1	FRAC2
$S_{0 \text{ at } 100 \text{ cycles AND } 30 \text{ Hz}}$	MPa	4138	4525	4016
Strain at 10^6 cycles	µm/m	142	140	161
N_{fat} at 100 µm/m	cycles	4.00E+06	4.49E+06	1.13E+07
C1	-	33.30	35.74	39.71
C2	-	3.93	4.43	5.10
R^2	-	0.96	0.91	0.99

4.2.6 Thermal cracking resistance and fracture energy

The average values of failure temperature (T_F) and failure stress (σ_F) from TSRST on three replicates for each mixture are given in Table 17. It can be easily found that the mixture FRAC1 has worse thermal cracking behaviour respect to the corresponding reference mixture, especially on the failure stress. However, when the binder content is adjusted, a much better thermal cracking behaviour can be achieved.

Table 17. Results of the TSRST.

Mixture	Failure Temperature T_F [°C]	Failure Stress σ_F [MPa]
Control	-26.2	3.763
FRAC1	-24.5	2.316
FRAC2	-28.2	3.474

Regarding the SCB tests, a single testing temperature of -18 °C was applied for each mixture, very good repeatability is found between each sample. In Table 18, the calculated nominal stress, σ_{max}, fracture energy, G_F, and fracture toughness, K_{IC} for are summarized. In Figure 21, the curves of the nominal stress vs. relative CMOD for these three different AC mixtures are illustrated, almost the same curves are observed between three materials in AC mixtures. However, overall higher values can be found in the materials prepared without fibre in Table 18. It is to say that materials without fibre have slightly better fracture resistance than the one prepared with fibres. However, the differences can be mitigated by adjusting the binder content. Based on the results, when a higher binder content is used for the AC mixture, a remarkable improvement on the thermal cracking properties can be obtained.

Table 18. SCB calculated parameters for surface layers at -18 °C.

Mixtures	σ_{max} [MPa]	G_F [J/m^2]	K_{IC} [MPa*m$^{1/2}$]
Control	4.305	1.074	31.780
FRAC1	3.654	0.877	26.986
FRAC2	3.955	0.950	29.507

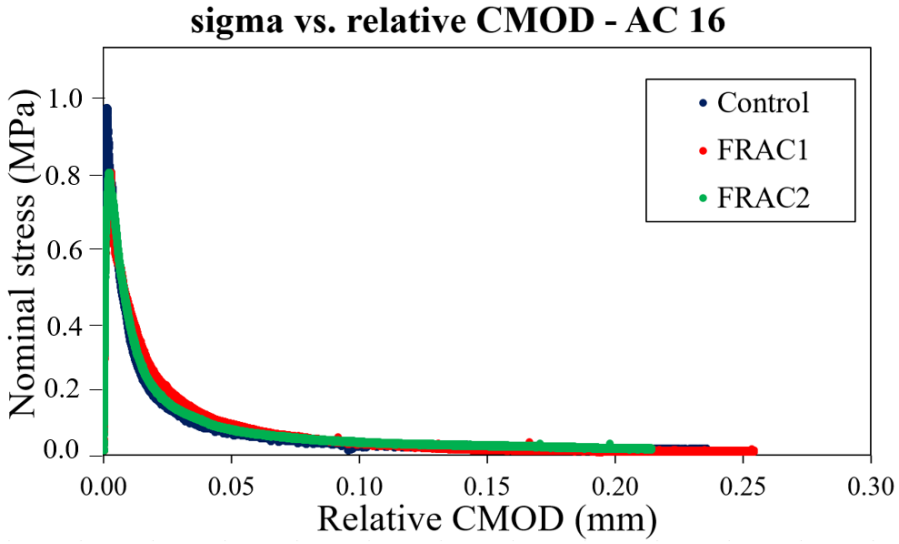

Figure 21. Comparison curves of different samples in T2.

4.3 Results on the AC mixtures for binder and base layers with and without fibres

4.3.1 Water sensitivity

The results of the water sensitivity tests in terms of the indirect tensile strength (ITS) in dry and wet conditions are illustrated in Figure 22. It can be seen that the asphalt mixtures prepared with fibres (B2, B5, T2) result in a higher ITS compared to the ones without fibres (B1, B4, T1) in dry condition. In the case of wet condition, B2 is still higher than B1; however, it is not true for binder layer with RAP and base layer mixtures. The highest ITS value was found for the mixture composed with RAP (B4 and B5). It can be clearly observed the influence of the incorporation of fibres on the strength which could be attributed to a reinforce effect in the experimental FRAM.

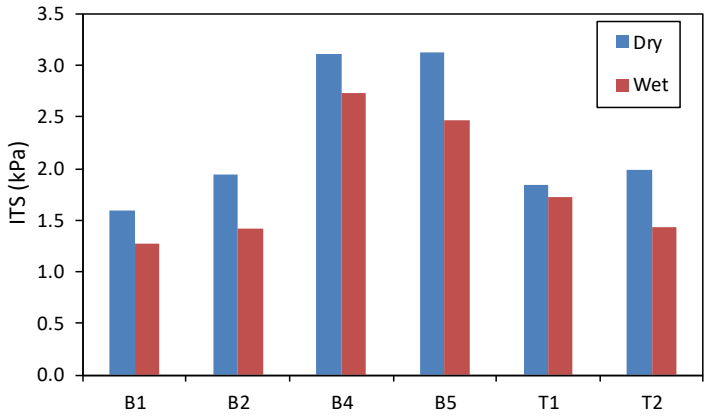

Figure 22. Indirect Tensile Strenght (ITS) results.

The water sensitivity results in terms of ITSR are shown in Figure . It can be observed that the T1 mixture prepared with the plain 50/70 bitumen showed the best moisture resistance capability, followed by the reference mixture with RAP and PMB (B4). All the mixtures containing fibres show worst moisture resistance capability, however all the FRAM mixtures fulfil the normative requirements of ITSR by reaching rates higher than 70%, which indicates reliable moisture distress resistance.

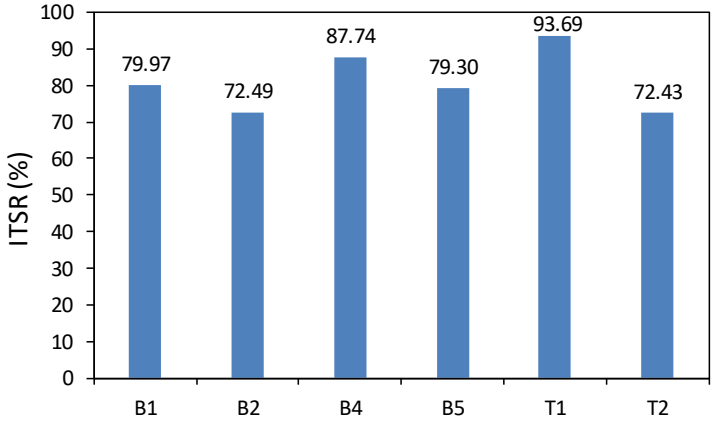

Figure 23. ITSR results.

4.3.2 Stiffness

In Figure 24 are illustrated the master curves of the complex modulus and of the phase angle at a reference temperature of 10°C for both the mixtures B1 and B2 of the binder layer. In Figure 25 are reported the master curves for the mixtures T1 and T2 of the base layer.

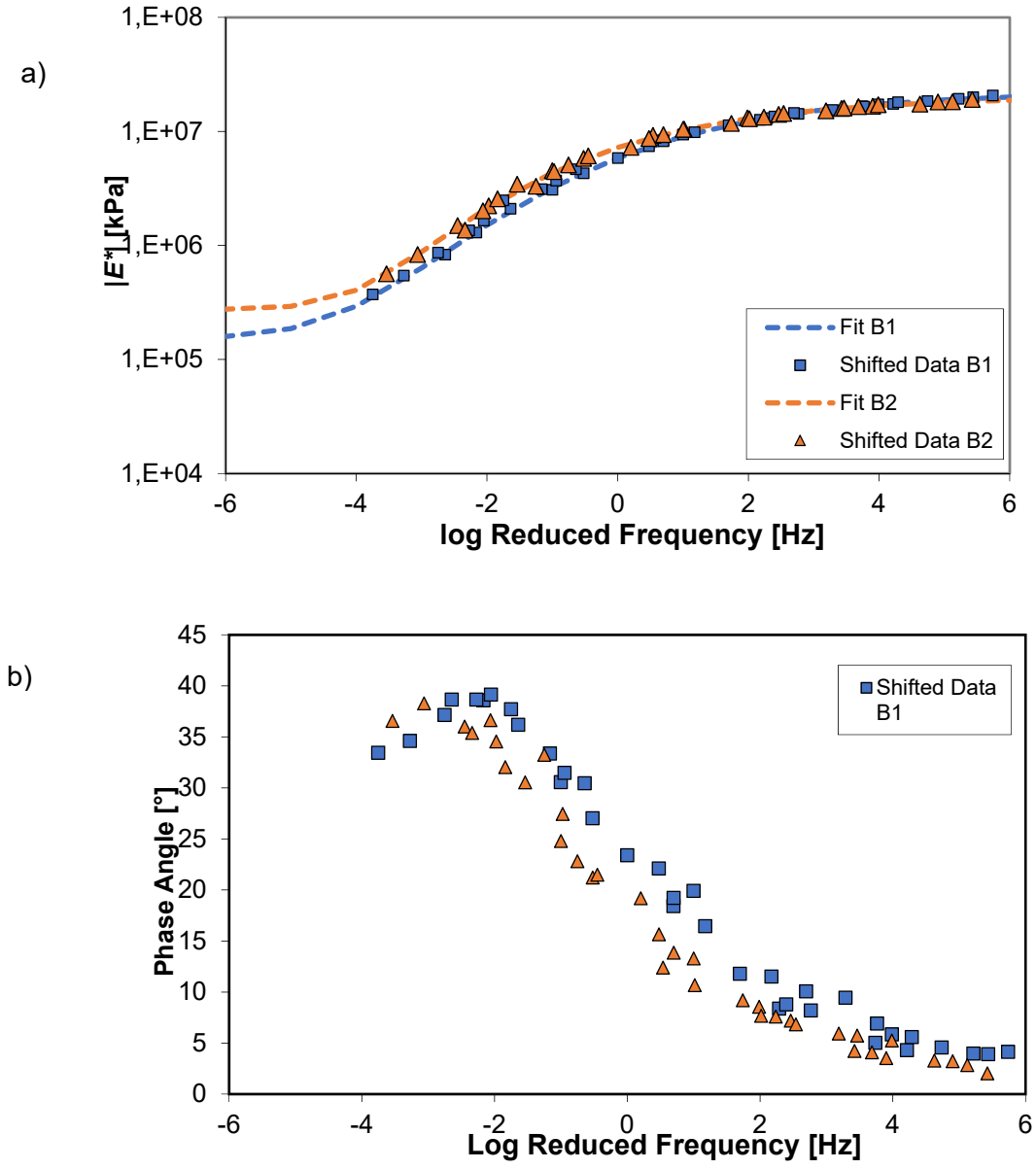

Figure 24. Master curves of a) the complex modulus; b)the phase angle for the binder mixtures B1 and B2 at a reference temperature of 10°C.

a)

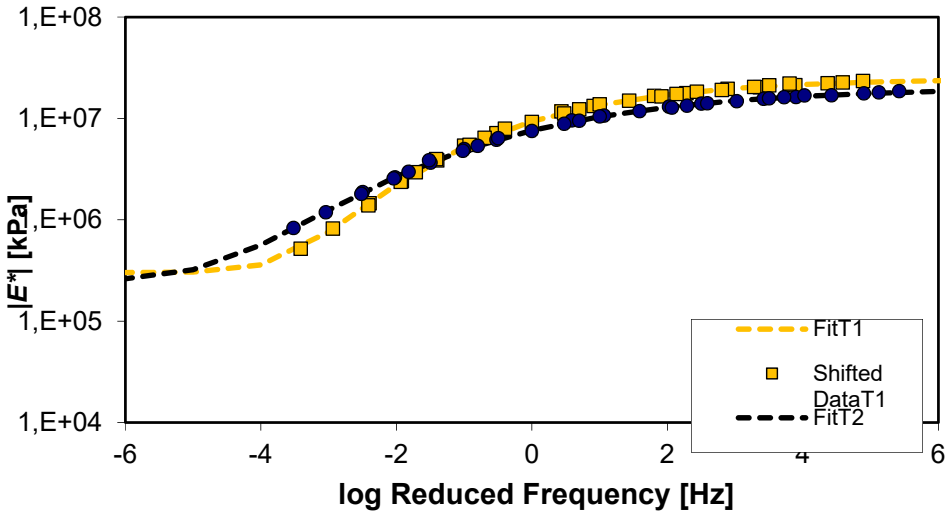

b)

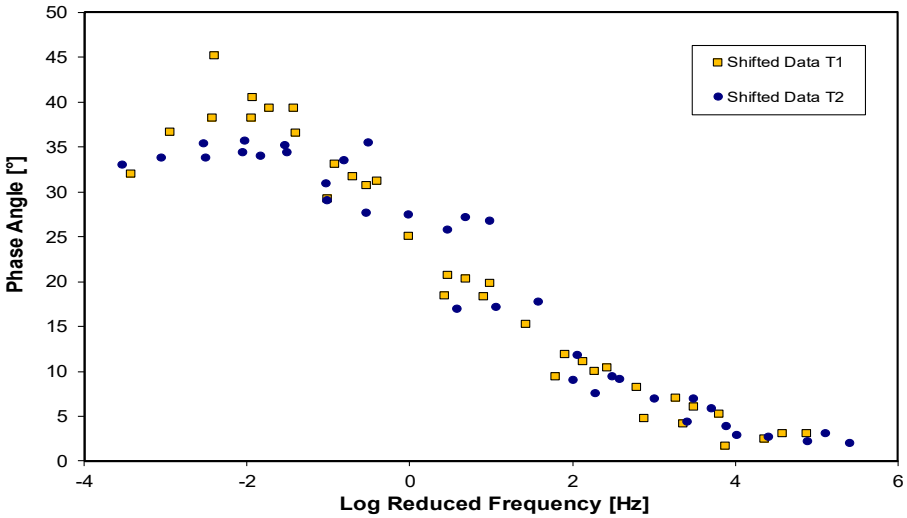

Figure 25. Master curves of a) the complex modulus; b) the phase angle for the base mixtures T1 and T2 at a reference temperature of 10°C.

In Table 19, the parameters of the master curves are summarized.

Table 19. Parameters of the master curves.

Parameters	B1	B2	T1	T2
E_e (kPa)	1.51×10^{5}	2.75×10^{5}	1.49×10^{5}	2.49×10^{5}
E_g (kPa)	2.20×10^{7}	2.03×10^{7}	2.20×10^{7}	2.02×10^{7}
f_c (Hz)	0.0127	5.156×10^{-6}	0.0139	2.142×10^{-5}
K (-)	0.20	0.19	0.25	0.18
m_e(-)	0.784	2.123	0.701	1.322
δ_m	37.52	40.37	38.66	35.24
f_d (Hz)	0.0013	6.158×10^{-5}	0.0014	0.0076
R_d (-)	1457.85	1717.75	1434.65	1506.25
m_d (-)	19842.2	24013	19987	27035
C_1	64.89	51.98	64.89	51.57
C_2	433.5	378.6	433.5	374.7

As shown in previous figures and table, very similar results for both the complex modulus and the phase angle were obtained for the binder mixtures B1 and B2 and for the base mixtures T1 and T2. Slightly higher complex modulus and lower phase angle at low frequencies (high temperatures range) and slightly low complex modulus and lower phase angle at high frequency (low temperatures range) for FRAM (B2 and T2) can be observed, indicating better mechanical properties for the mixtures containing fibres. This means that, in the linear viscoelastic range, the mechanical behaviour of mixes B2 and T2, formed by fibres and pen grade bitumen 50/70 and 35/50 respectively, is similar or even better than the corresponding reference mixtures B1 and T1 composed with PMB 45/80-65 and 50/70 pen binder respectively. Therefore, the mechanical properties of a polymer-modified binder can be reached or even improved adding fibres to plain binder.

4.3.3 Rutting resistance

In Table 20, the results of the wheel tracking tests in terms of rut depth and slope of the curve at 1000 cycles are summarized for the binder mixtures B1 and B2 and for the base mixtures T1 and T2. It can be observed that, the FRAM mixture B2 has a slightly worsen rutting performance showing a higher slope and higher rut depth respect to the polymer modified mixtures B1. However, both mixtures present an excellent rutting resistance, largely respecting the standard requirements for binder layer mixtures. Regarding the mixtures T1 and T2 of the base layer, the FRAM mixture T2 shows better rutting performance compared to the reference mixture T1.

Table 20. Results of rutting tests for binder layer mixtures.

	B1	B2	T1	T2
Slope (mm/1000 cycles)	0.016	0.021	0.036	0.009
Rut depth (mm)	1.42	2.15	2.89	1.70
Rutting depth (%)	3.2	3.5	4.4	2.5

4.3.4 Fatigue resistance

Figure 26 and Figure 27 display the testing results on the mixtures for the binder and base layers based on the fatigue experimental measurements according to the European standard EN12697-24. Five different stress levels, summarized in Table 21, were used for each mixture. In Figure 26 and Figure 27, the Wohler curves with the fatigue law and the initial stiffness obtained at the same stress levels are reported.

Table 21. Stress levels applied for the fatigue tests.

	σ_0 [MPa]
B1	0.40, 0.35, 0.30, 0.25, 0.20
B2	0.35, 0.25, 0.20, 0.15, 0.10
T1	0.50, 0.60, 0.70, 0.80, 0.90
T2	0.40, 0.50, 0.60, 0.70, 0.80

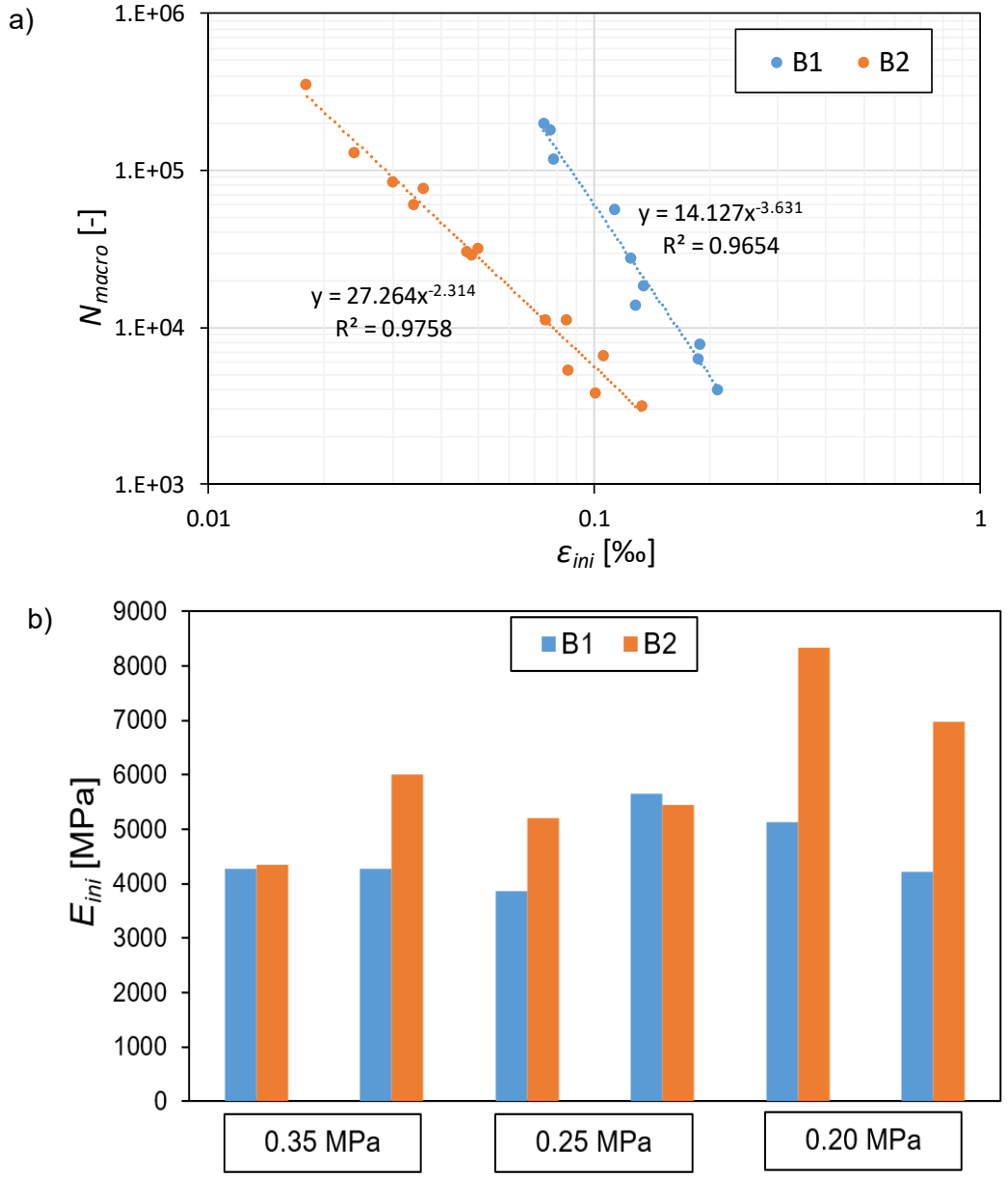

Figure 26. Fatigue results for the mixtures of the binder layer at f=10 Hz and at 20°C: a) loading cycles to fatigue failure Nmacro vs initial strain level; b) initial stiffness

As shown in Figure 26, good repeatability of the test was achieved at each stress levels, in fact the fatigue lines have a high correlation coefficient R^2, greater than 0.9 satisfying the requirements of the standard for the binder layer. The FRAM mixture B2 might have better fatigue response for higher strain levels, since the slope of the fatigue line is higher than the one of the PmB mixture. In the studied strain levels, the fatigue line of the FRAM mixture B2 is lower than that of the PmB mixture B1, indicating a worse fatigue performance. In fact, at the same initial strain, a smaller number of cycles are needed to induce fatigue damage. Therefore, for lower strain levels, FRAM mixture does not reach the performance of the reference PmB mixture. This can be due to the much higher initial stiffness observed for the FRAM mixture in comparison to the values of the reference mixture (Figure 14b).

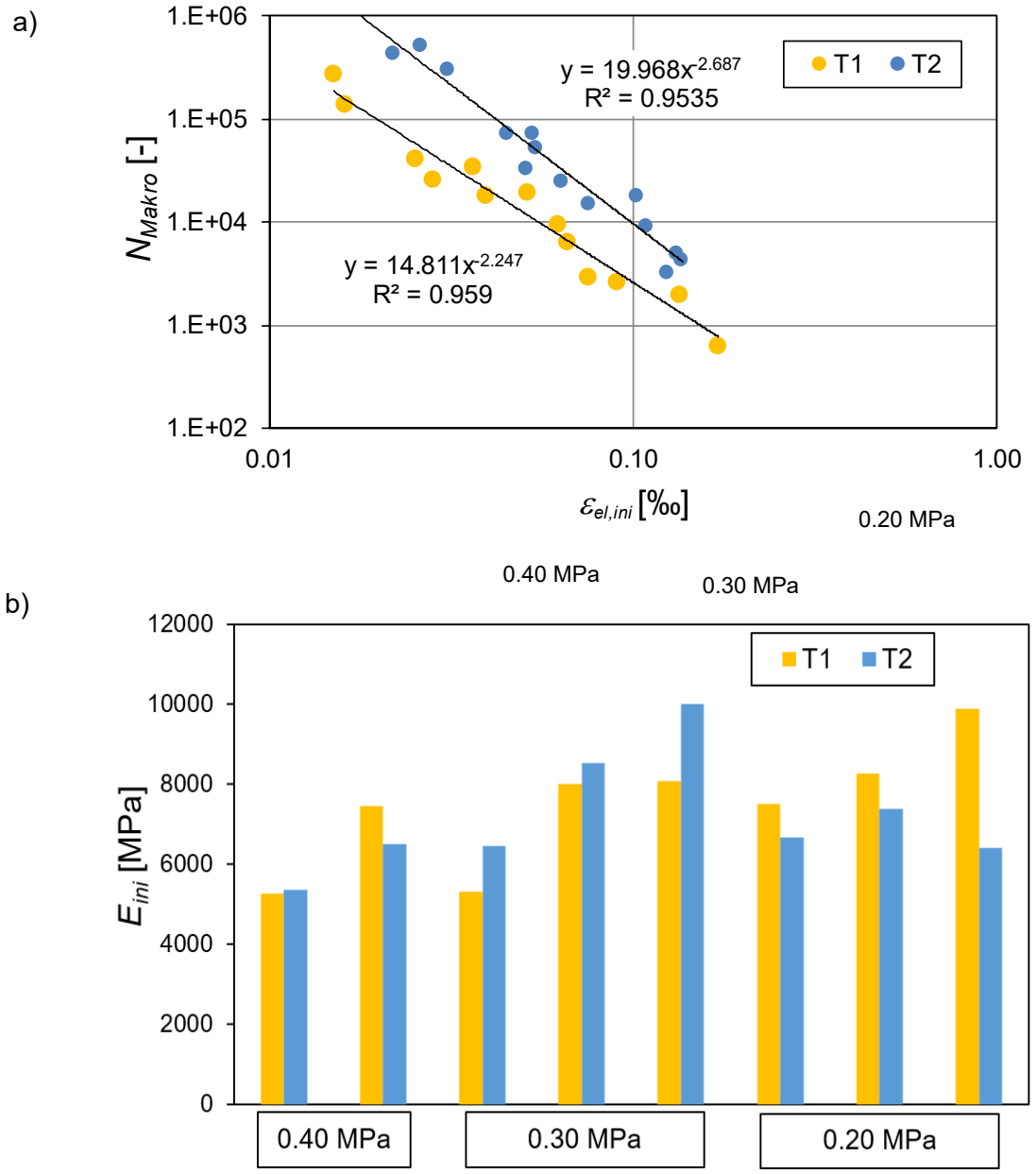

Figure 27. Fatigue results for the mixtures of the base layer at f=10 Hz and at 20°C: a) loading cycles to fatigue failure Nmacro vs initial strain level; b) initial stiffness

As shown in Figure 27, the FRAM T2 shows better fatigue performance compared to the reference mixture T1. In addition, very good repeatability of the tests can be observed, in fact the R^2 is greater than 0.9, higher than the requirement of the standards for the base layer, where R^2 should be greater than 0.8. Therefore, the addition of fibres to a mixture composed with plain 35/50 binder can lead to reach and even improve the fatigue performance of a mixture composed with plain 50/70 binder.

4.3.5 Thermal cracking resistance and fracture energy

The average values of failure temperature (T_F) and failure stress (σ_F) from TSRST on three replicates for each mixture are given in Table 22. Figure 28 shows mean cryogenic stress (σcry) versus temperature for the mixtures of the binder layer, and **¡Error! No se encuentra el origen de la referencia.** show the results of the mixtures of the base layer.

Table 22. Results of the TSRST.

Mixture	Failure Temperature T_F [°C]	Failure Stress σ_F [MPa]
B1	-29.5	4.687
B2	-21.4	2.655
T1	-22.5	2.777
T2	-17.4	2.073

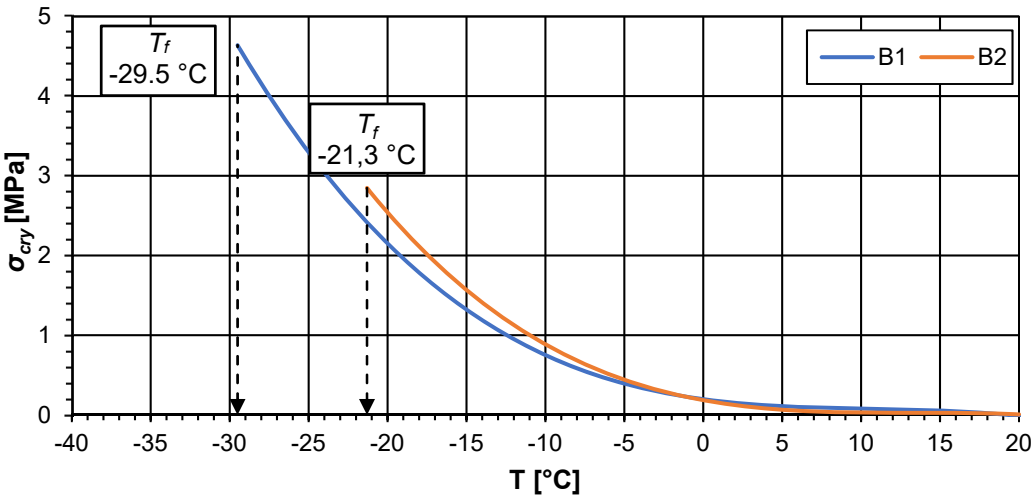

Figure 28. TSRST results: mean cryogenic stress σcry(T) versus temperature for the mixtures of the binder layer.

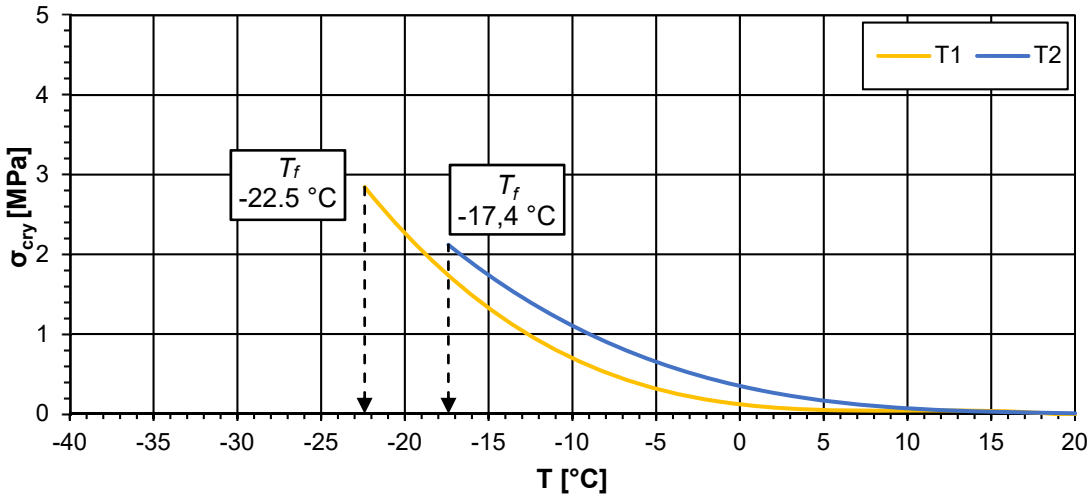

Figure 29. TSRST results: mean cryogenic stress σcry(T) versus temperature for the mixtures of the base layer.

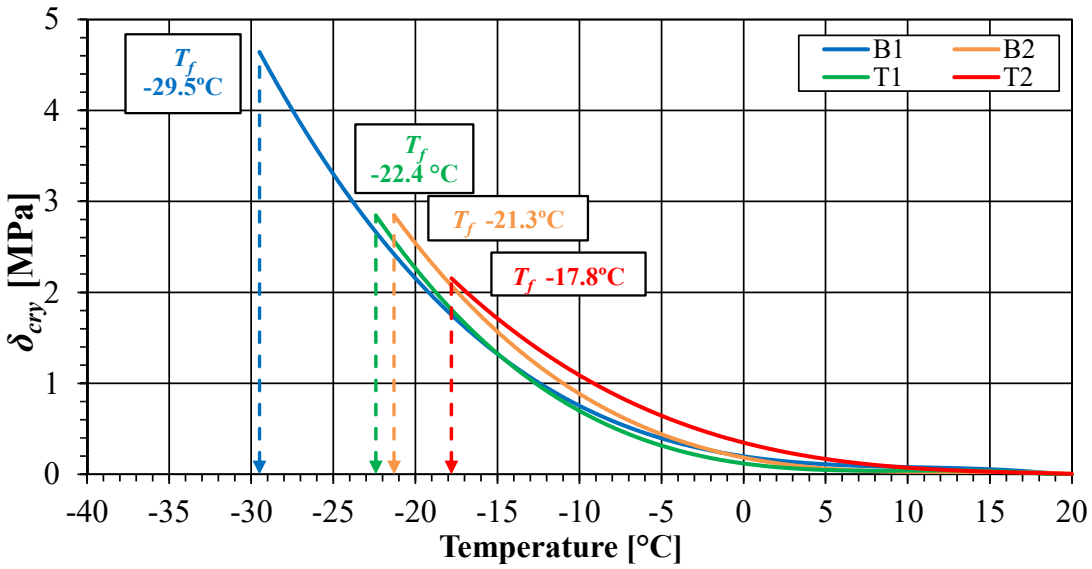

Figure 30. TSRST results: mean cryogenic stress σcry(T) versus temperature for the mixtures of the binder and base layer.

As shown in the previous figures and table, the FRAM mixture for both the binder (B2) and base layers (T2) has a worse thermal cracking behaviour respect to the corresponding reference mixture (B1 and T1). The difference between the failure temperatures of the two mixtures is 8.2 °C for the mixtures of the binder layer and circa 5°C for the mixtures of the base layer. However, comparing the results of B2 and T1 with the same bitumen and similar characteristics (percentage bitumen and void content), the low temperature performance is very similar, indicating an almost null effect of the fibres on this parameter.

Finally, based on the German requirements for binder and base layers (Table 23), B1 and T1 mixtures can be used in cold region Class III, while the B2 and T2 mixtures can be used in cold region Class II.

Table 23. German requirements for binder and base layers

Frosteinwirkungszone nach RStO 01	Asphaltbeton für Asphaltdeckschichten und Asphaltbinder	Asphalttragschichtmischgut
I	$T_{Br} \leq -15$ °C	$T_{Br} \leq -10$ °C
II	$T_{Br} \leq -20$ °C	$T_{Br} \leq -15$ °C
III	$T_{Br} \leq -25$ °C	$T_{Br} \leq -20$ °C

Regarding the SCB tests, a single testing temperature of -18 °C was applied for all the mixtures. In Figure 31, the curves of the nominal stress vs. relative CMOD for three different samples of T2 mixture is illustrated. Very good repeatability can be observed for both T1 and T2 mixtures. It is to say that mixtures containing fibres can achieve similar homogenous results compared to the conventional asphalt mixture.

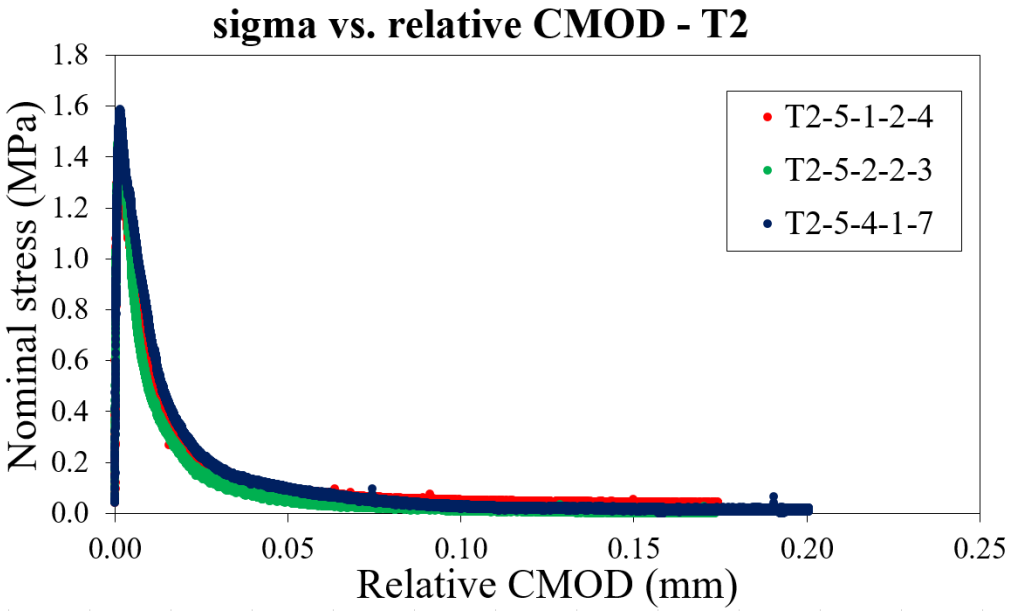

Figure 31. Comparison curves of different samples in T2.

In Table 24 the calculated nominal stress, σmax, fracture energy, GF, and fracture toughness, KIC for the mixtures of the binder and base layers are summarized. It can be seen that B1 has higher σmax and the related GF compared to B2, while a lower KIC was obtained at the same time. It is to say that B1 can undergo a higher load compared to B2 which will ultimately lead to a higher fracture energy; however, when the initial cracking occurs, the cracks are easier to propagate in B1. Hence, it can be concluded that mixtures prepared with unmodified 50/70 bitumen together with fibres have less fracture energy at low temperature, but the reaction between fibres and mixtures can lead to a softer material. To better understand the thermal behaviour of these two materials, the corresponding comparison curves are illustrated in Figure 32. Very similar after peak slope was found between B1 and B2, it is noting that both materials have similar brittle properties.

In the case of the base mixtures T1 and T2, as can be observed from the parameters reported in Table 24 and from the curves in Figure 33, there are almost no differences between these two materials. In addition, as before, if B2 is compared with T1, no significant differences are neither observed. Therefore, in this case, it seems that the use of a lower penetration grade bitumen or the addition of fibres do not have an important effect of this parameter.

Table 24. SCB calculated parameters for binder and base layers at -18 °C.

Mixtures	σ_{max} [MPa]	G_F [J/m^2]	K_{IC} [MPa*m$^{1/2}$]
B1	3.830	1.171	27.998
B2	2.613	0.484	19.691
T1	2.708	0.430	20.254
T2	2.762	0.391	20.246

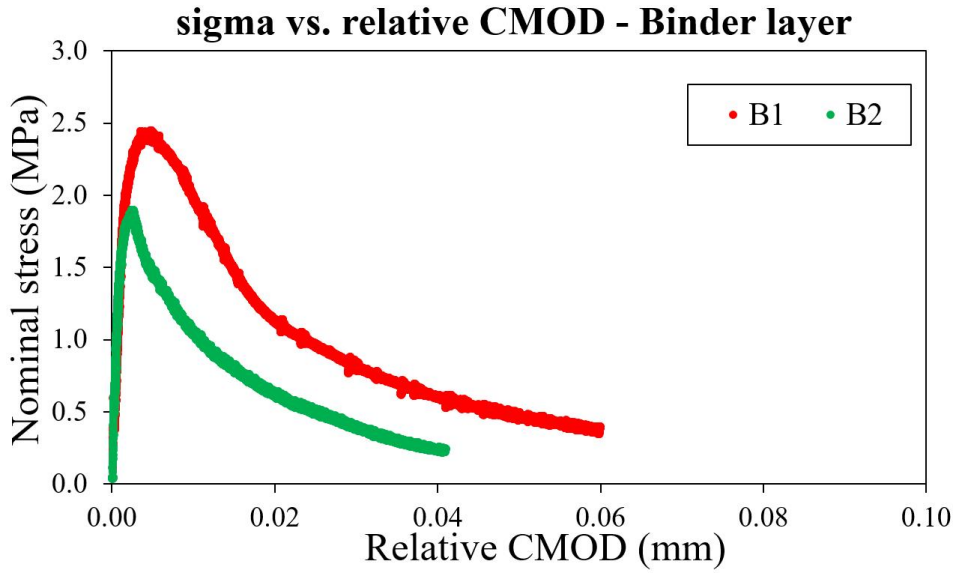

Figure 32. Curve comparison between B1 and B2 for binder layer mixture.

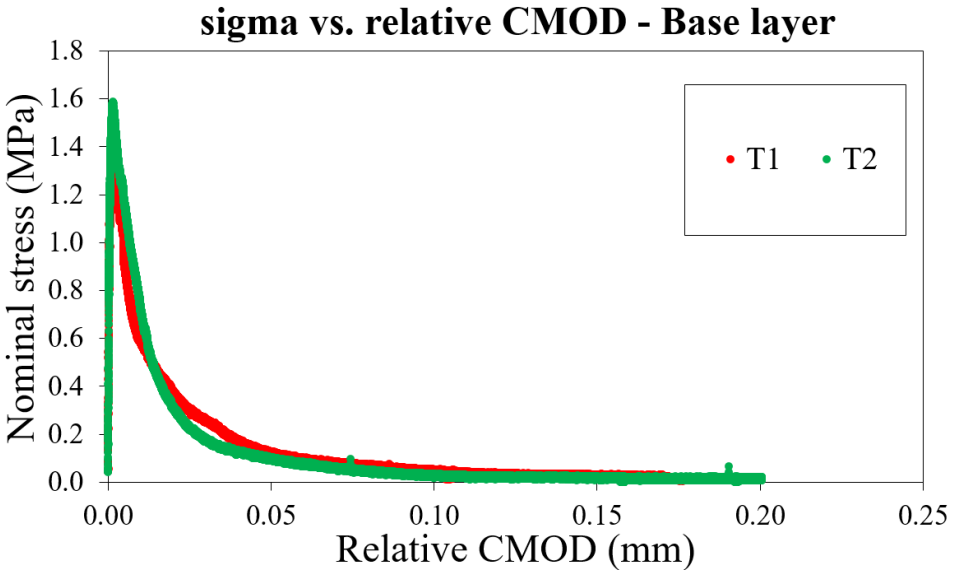

Figure 33. Curve comparison between T1 and T2 for base layer mixture

4.4 Results on AC mixtures for the surface layer with 50% artificially aged fibre-reinforced RAP (PANRAP)

4.4.1 Bulk density and air voids

Table 25 presents the results concerning density and air voids in the mixtures prepared with PANRAP. Once the volumetric properties were measured, the same specimens served as the basis for calculating the flow and the Marshall Stability. Mixtures manufactured with PANRAP showed lower air void content in comparison to the control and plain FRAC mixes. However, the void content in the mixes was kept between 4.00% and 6.00%, which is adequate for surface layers. In terms of Marshall Stability and Flow values, not significant changes were observed between them and concerning control and FRAC mixes.

Table 25. Bulk density and air void results

Bulk density and voids EN 12697 - 8	Units	Control-PANRAP		FRAC-PANRAP	
		Mean	SD	Mean	SD
Density	g/cm3	2.45	0.01	2.45	0.01
Voids in mixture	(%)	4.41	0.27	4.47	0.20
Voids in aggregates	(%)	13.49	0.25	13.55	0.19
Marshall Stability	kN	15.56	0.64	14.73	0.67
Flow	mm	3.32	0.52	3.39	0.17

4.4.2 ITS and moisture sensitivity results

The results of ITS in both dry and wet conditions, as well as the ITSR, are presented in Figure 31Figure . From the results, it can be seen that both mixes increased considerably the ITS in dry and wet conditions as compared to control and FRAC mixes (Figure 18). Regarding the addition of type P fibres in the mixtures prepared with PANRAP, there is an increment also in the tensile strength response. Accordingly, the reinforcing effect of fibres is also useful when recycled FRAC mixture is incorporated. Concerning the ITSR value, both mixes presented similar values of moisture resistance capability by reaching rates higher than the 85%.

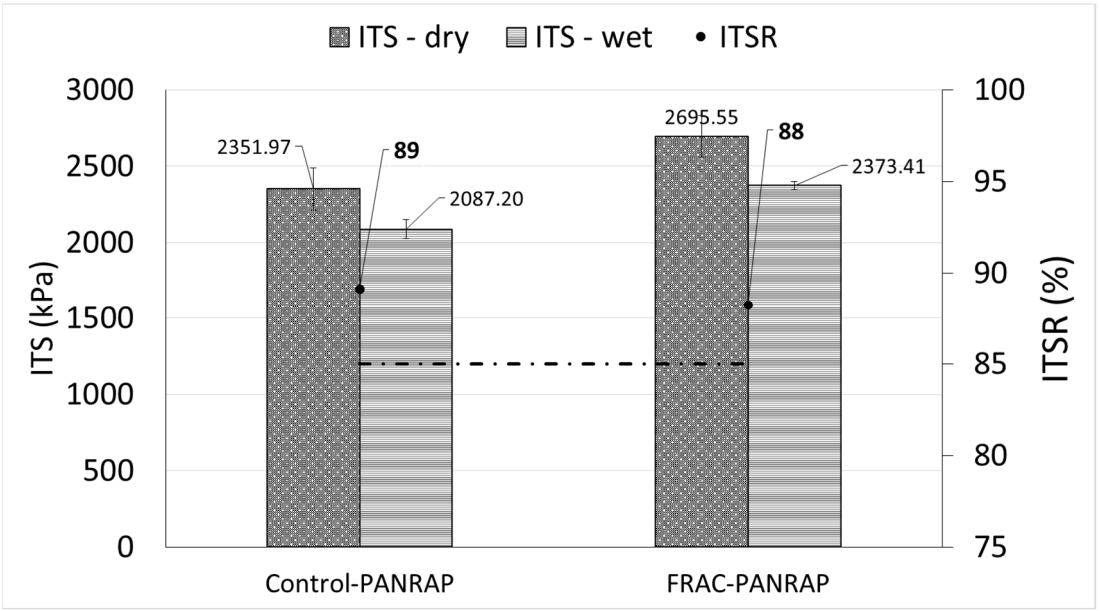

Figure 34. ITS and moisture sensitivity results of AC mixtures with PANRAP

4.4.3 Rutting

Table 26 displays the results obtained from the wheel tracking test. Both mixtures with PANRAP performed well, giving good results in the resistance to permanent deformation even better as compared to the control mixture (Table 15). Besides, the FRAC-PANRAP mixture reported a better rutting resistance than Control – PANRAP mixture since the rutting depth after 10000 cycles, as well as the slope values, were lower.

Table 26. Rutting results of AC mixtures with PANRAP

Wheel tracking test EN 12697 - 22	Units	Control-PANRAP		FRAC-PANRAP	
		Mean	SD	Mean	SD
Slope	mm/1000 cycles	0.05	0.02	0.03	0.01
Rutting depth	mm	2.30	0.70	1.80	0.30

4.4.4 Stiffness

From the stiffness test, the dynamic modulus, as well as the phase angle, were registered at different levels of frequencies, as shown in Figure 35. From the results, it can be observed that mixtures manufactured with PANRAP displayed higher dynamic modulus and lower phase angle as compared to control and FRAC mixes (Figure 19). Due to the presence of artificial RAP, the mixtures become stiffer making them more elastic. Similar results were observed in terms of dynamic modulus and phase angle between Control-PANRAP and FRAC-PANRAP mixes.

(a)

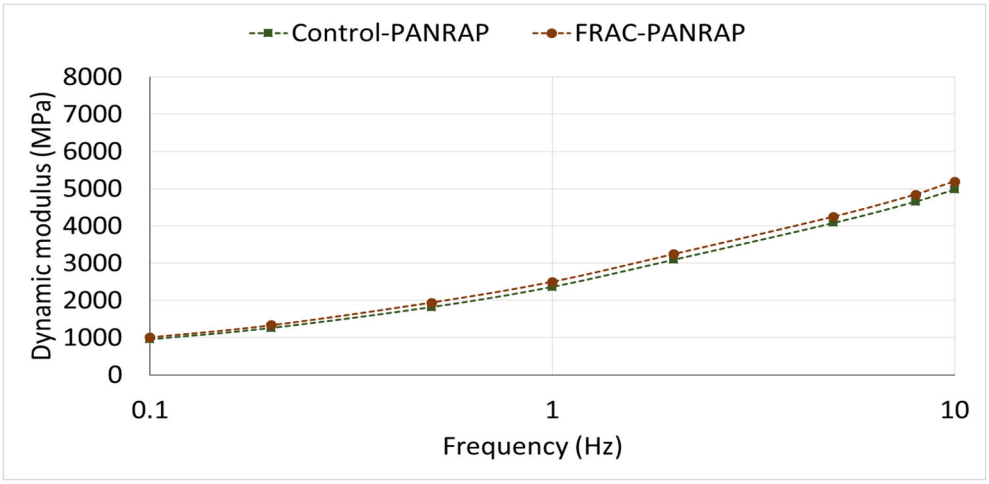

(b)

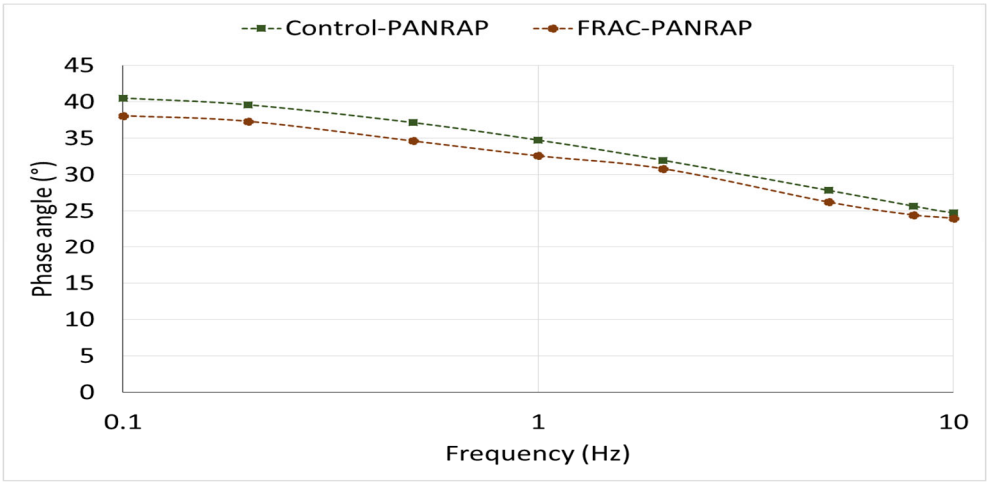

Figure 35. Dynamic modulus and phase angle of AC mixtures with PANRAP

4.4.5 Fatigue resistance

Figure 36 and Table 27 illustrate the fatigue curves and the main parameters obtained from the fatigue resistance test. Both fatigue laws displayed R^2 values greater than 0.8, indicating a good correlation. From the results, it can be seen that Control-PANRAP mixture showed higher fatigue resistance at high strain levels. Nevertheless, at lower strain levels, the behavior is almost the same, indicating similar fatigue resistance. However, the initial modulus of the FRAC-PANRAP mix was still higher in comparison to the control mixture with aged fibre-reinforced RAP.

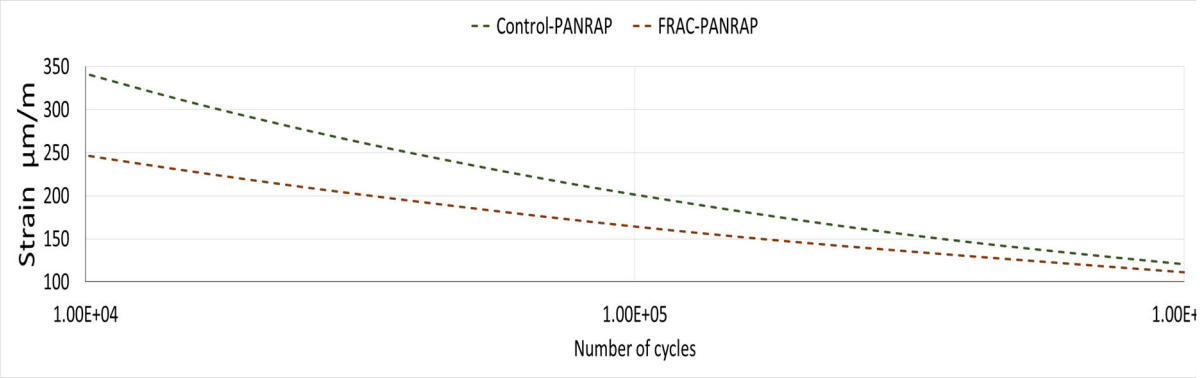

Figure 36. Fatigue resistance results of AC mixtures with PANRAP

Table 27. Main parameters obtained from the fatigue resistance test

Parameter	Unit	Control-PANARAP	FRAC-PANARAP
$S_{0 \text{ at } 100 \text{ cycles AND } 30 \text{ Hz}}$	MPa	6362	7236
Strain at 10^6 cycles	µm/m	119	110
N_{fat} at 100 µm/m	cycles	2.14E+06	1.71E+06
C_1	-	34.69	40.54
C_2	-	4.37	5.69
R^2	-	0.92	0.85

4.4.6 Thermal cracking resistance and fracture energy

The average values of failure temperature (T_F) and failure stress (σ_F) from TSRST on three replicates for each mixture are given in Table 28. Similar thermal cracking behaviour can be found in two mixtures.

Table 28. Results of the TSRST.

Mixture	Failure Temperature T_F [°C]	Failure Stress σ_F [MPa]
Control-PANRAP	-22.3	3.373
FRAC-PANRAP	-21.5	3.549

Regarding the SCB tests, a single testing temperature of -18 °C was applied for each mixture, very good repeatability is found between each sample. In Table 29, the calculated nominal

stress, σ_{max}, fracture energy, G_F, and fracture toughness, K_{IC} for are summarized. In Figure 37, the curves of the nominal stress vs. relative CMOD for these two different mixtures containing artificial aged fibre-reinforced RAP are illustrated. In both Table 29 and Figure 37, worse fracture resistance response, σ_{max} and K_{IC}, are observed in FRAC-PANRAP. In the case of fracture energy, materials prepared with fibres gain higher G_F compared to the ones without fibres. Hence, it is to say that the use of fibre improves the low temperature fracture resistance properties.

Table 29. SCB calculated parameters for binder and base layers at -18 °C.

Mixtures	σ_{max} [MPa]	G_F [J/m^2]	K_{IC} [MPa*m$^{1/2}$]
Control-PANRAP	3.768	0.736	28.300
FRAC-PANRAP	2.846	0.871	21.335

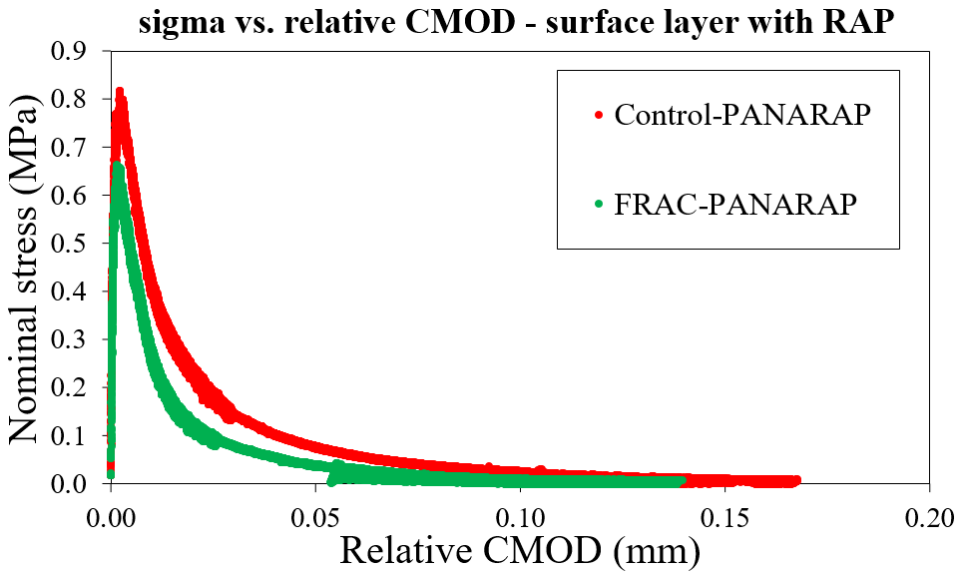

Figure 37. Curve comparison between T1 and T2 for base layer mixture

4.5 Results on AC mixtures for surface layer 30% real RAP with and without fibres

4.5.1 Bulk density and air voids

The results concerning the bulk density and the air voids are presented in Table 30. Similarly, the Marshall Stability and the flow were determined once the volumetric properties were measured. Although Control - 30% RAP and FRAC - 30% RAP showed the same flow value, the Marshall Stability was slightly higher in the design with fibres incorporated.

Table 30. Bulk density and voids results of AC mixtures with RAP

Bulk density and voids EN 12697 - 8	Units	Control-30%RAP		FRAC-30%RAP	
		Mean	SD	Mean	SD
Density	g/cm^3	2.43	0.01	2.45	0.00
Voids in mixture	(%)	4.92	0.33	4.04	0.18
Voids in aggregates	(%)	13.13	0.30	12.33	0.17
Marshall Stability	kN	13.85	0.77	14.95	0.23
Flow	mm	5.51	1.75	5.51	0.46

4.5.2 Indirect tensile strength and moisture sensitivity

The ITS results of both dry and wet conditions, as well as ITSR, are depicted in Figure 38. Although both mixtures presented a suitable moisture resistance since the ITSR value rates higher than the 85%, the FRAC – 30%RAP presented greater ITSR and also performed better ITS values in both dry and wet conditions, suggesting a positive effect of the added fibre.

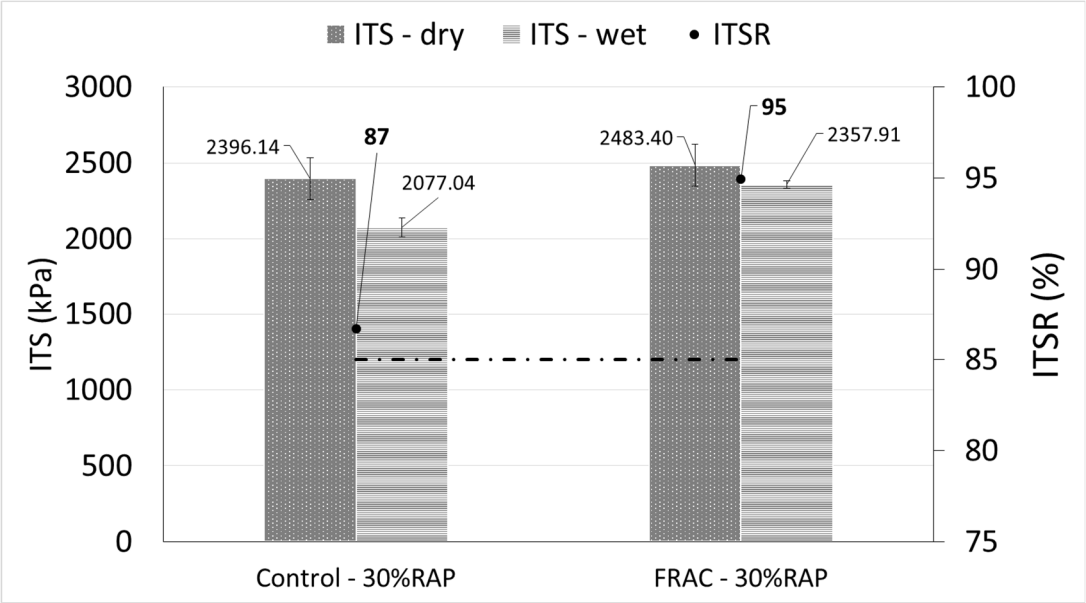

Figure 38. ITS and moisture sensitivity results of AC mixtures with 30% RAP

4.5.3 Rutting

Table 31 displays the results obtained from the wheel tracking test. From the test, the linear slope (mm/1000 cycles) was calculated per each mixture as well as the rut depth (mm) once 10.000 load cycles were reached. As can be seen in the table, both mixes present a proper rutting resistance.

Table 31. Rutting results of AC with RAP

Wheel tracking test EN 12697 - 22	Units	Control - 30% RAP		FRAC - 30% RAP	
		Mean	SD	Mean	SD
Slope	mm/1000 cycles	0.03	0.01	0.03	0.00
Rutting depth	mm	2.17	0.15	2.23	0.55

4.5.4 Stiffness

From the stiffness test, the dynamic modulus, as well as the phase angle, were registered at different levels of frequencies, as can be seen in Figure 39. Both mixes with RAP displayed approximately the same dynamic modulus and phase angle for the different range of frequencies. Although the addition of fibres could stiffen the FRAC- 30%RAP mixture in a greater proportion than the Control – 30% RAP, not significant changes were observed for both responses. These mixtures show higher stiffness modulus due to the addition of RAP and the use of conventional 50/70 penetration grade binder.

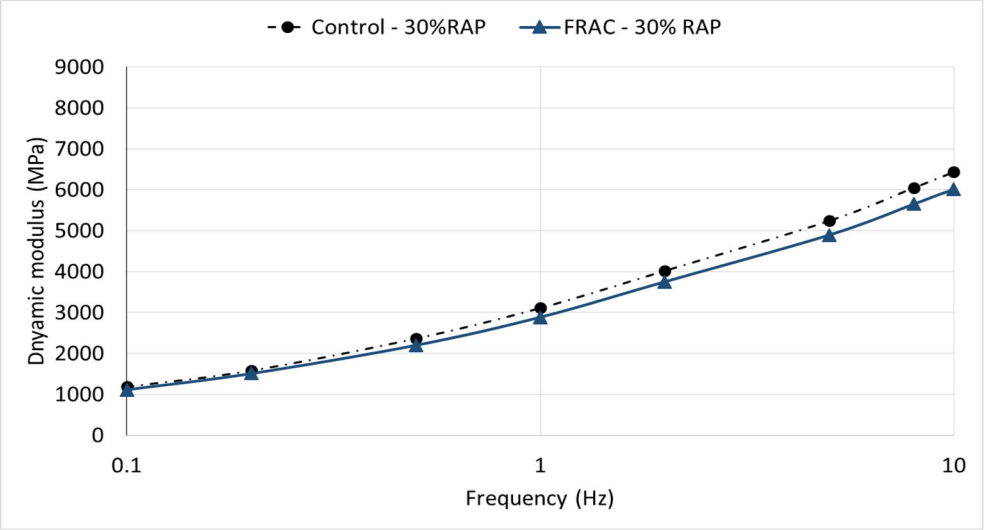

(a)

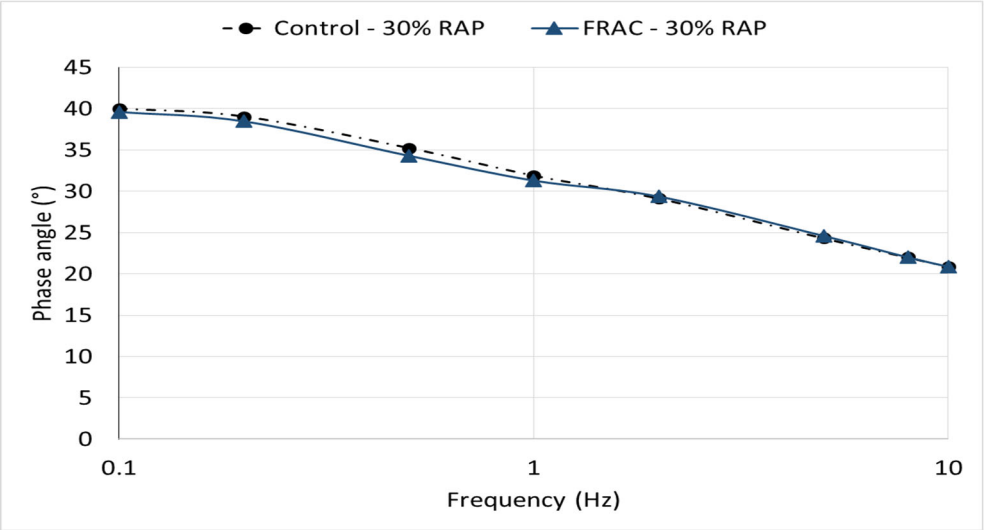

(b)

Figure 39. Stiffness test results of AC mixtures manufactured with RAP

4.5.5 Fatigue resistance

Figure 40 and Table 32 illustrate the behaviour against fatigue of both mixtures. Both mixtures show the highest variability with a R^2 values around 0.7 due to the incorporation or real RAP.

Its use with conventional binder 50/70 make the mixtures stiffer, which results in mixtures with lower fatigue resistance. In this case, the behaviour of both mixtures with or without fibres is very similar, so the impact of the RAP seems higher than the incorporation of fibres.

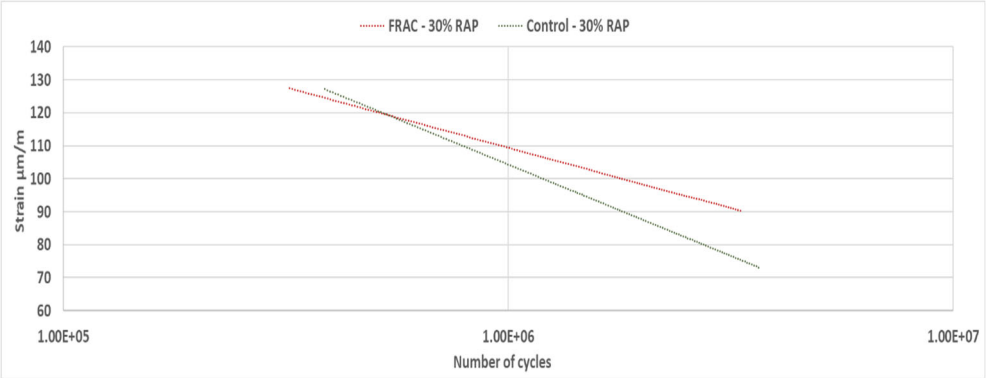

Figure 40. Fatigue resistance results of AC mixtures with PANRAP

Table 32. Main parameters obtained from the fatigue resistance test

Parameter	Unit	Control - 30% RAP	FRAC - 30% RAP
$S_{0 \text{ at } 100 \text{ cycles AND } 30 \text{ Hz}}$	MPa	8291.2	7980.4
Strain at 10^6 cycles	µm/m	104	109
N_{fat} at 100 µm/m	cycles	1.024E+06	1.36E+06
C1	-	26.68	36.70
C2	-	2.79	4.90
R^2	-	0.66	0.69

4.5.6 Thermal cracking resistance and fracture energy

The average values of failure temperature (T_F) and failure stress (σ_F) from TSRST on three replicates for each mixture are given in Table 33. A lower failure temperature and similar failure stress are achieved in the FRAM mixture. It is to say a relative better thermal cracking resistance can be gain by using fibre.

Table 33. Results of the TSRST.

Mixture	Failure Temperature T_F [°C]	Failure Stress σ_F [MPa]
Control - 30% RAP	-23.7	3.915
FRAC - 30% RAP	-25.1	3.817

Regarding the SCB tests, a single testing temperature of -18 °C was applied for each mixture, very good repeatability is found between each sample. In Table , the calculated nominal stress, σ_{max}, fracture energy, G_F, and fracture toughness, K_{IC} for are summarized. In Figure 41, the curves of the nominal stress vs. relative CMOD for these two different mixtures are illustrated. Very similar values and curves are found between different mixtures, it is to say that when only 30% of real RAP for mixture design, no remarkable influence can be caused by using fibre.

Table 34. SCB calculated parameters for binder and base layers at -18 °C.

Mixtures	σ_{max} [MPa]	G_F [J/m^2]	K_{IC} [MPa*m$^{1/2}$]
Control - 30% RAP	3.159	0.835	23.716
FRAC - 30% RAP	2.978	0.729	22.397

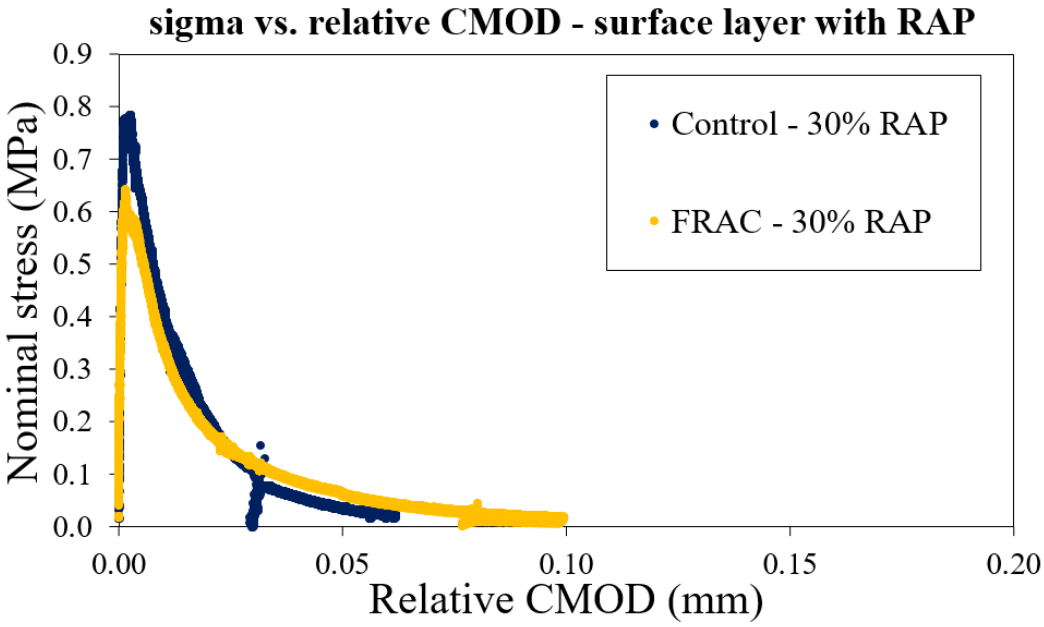

Figure 41. Curve comparison between B1 and B2 for binder layer mixture.

4.6 Results on AC mixtures for binder layer with 50% real RAP content with and without fibres

4.6.1 Water sensitivity

As reported in Figure 20, the mixtures containing RAP have the highest value of ITS in both dry and wet condition compared to all the other mixtures. The B4 mixture composed with PmB and RAP presents an ITSR value of 87.7%, while the B5 mixture composed with binder 50/70, fibres and RAP presents an ITST value of 79.3%. Therefore, even if the FRAM mixture show worse moisture resistance capability, it fulfills the standard requirements.

4.6.2 Stiffness

In Figure 42 the master curves of the complex modulus and of the phase angle for the mixtures containing RAP are reported.

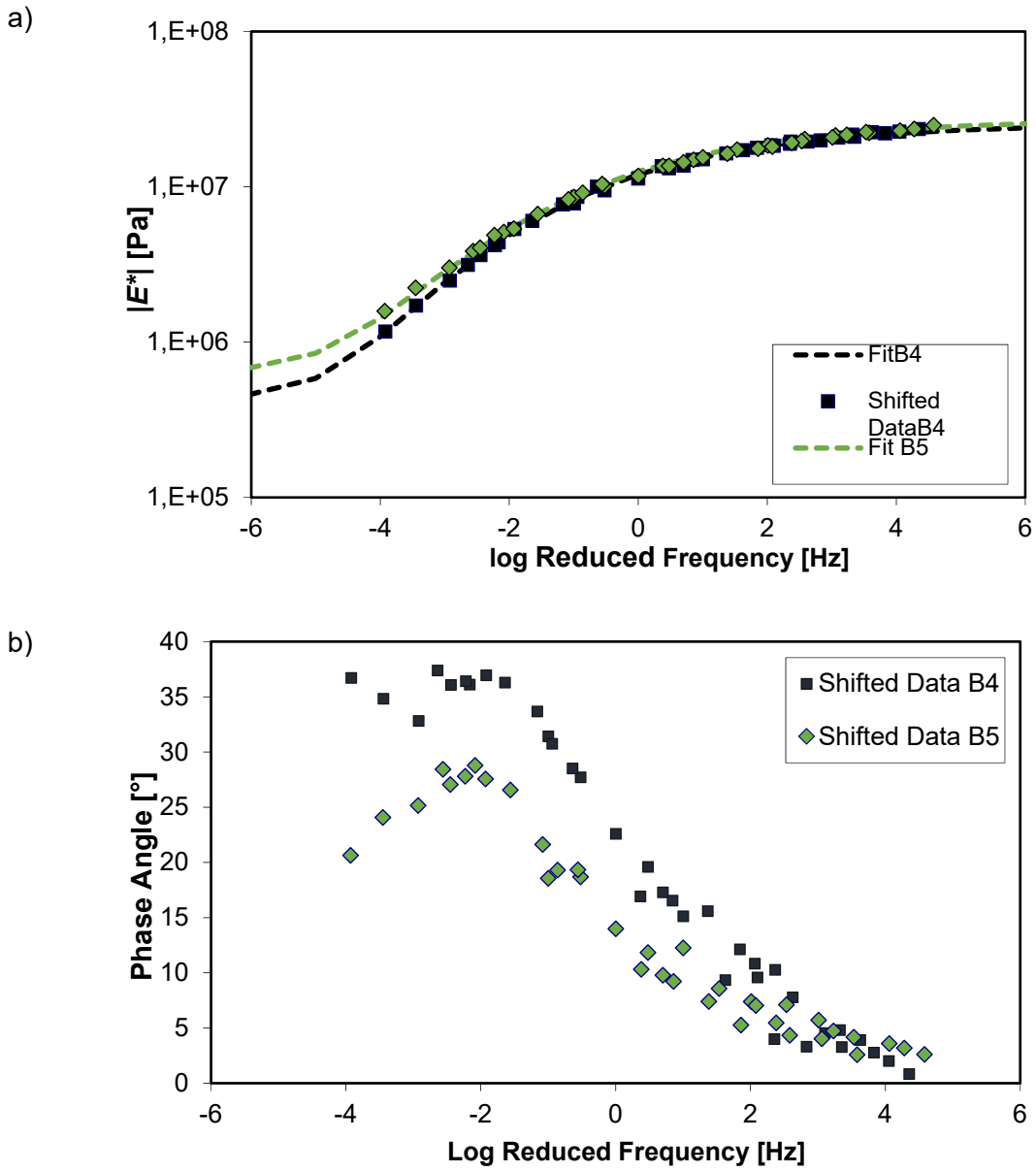

Figure 42. Master curves of a) the complex modulus; b) the phase angle for the binder mixtures with RAP B4 and B5 at a reference temperature of 10°C.

As shown in the previous figure, the complex modulus for the mixture with and without fibres, B4 and B5 respectively are very similar, while the phase angle of the mixture composed with RAP, 50/70 binder and fibres (B5) at lower frequencies (high temperatures) are much lower than the mixture composed with RAP and PmB binder. It indicates that the mixture containing fibres has a more elastic and less viscous behaviour especially in the high temperature range in comparison with the mixture B4. In addition, comparing these results with the mixtures B1 and B2 reported in Figure 22, it can be observed much higher complex modulus for B4 and B5, due to the presence of RAP binder in the mixtures. Table 35 summarized the parameters of the master curve.

Table 35. Parameters of the master curves of the mixtures containing RAP.

Parameters	B4	B5
E_e (kPa)	4.43×10^{5}	6.52×10^{5}
E_g (kPa)	2.54×10^{7}	2.73×10^{7}
f_c (Hz)	1.398×10^{-6}	1.569×10^{-6}
K (-)	0.18	0.17
m_e(-)	1.83	1.61
δ_m	36.91	26.25
f_d (Hz)	0.0014	0.0018
R_d (-)	1407.61	1279.73
m_d (-)	202009	24013
C_1	419.2	183
C_2	2899	1293

4.6.3 Rutting resistance

In Table 36 are summarized the results of the Wheel tracking tests for the mixture B4 and B5. Both the mixtures present very similar values indicating very good rutting performance.

Table 36. Rutting results on mixtures containing RAP.

	B4	B5
Slope (mm/1000 cycles)	0.011	0.014
Rut depth (mm)	1.64	1.58
Rutting depth (%)	2.2	2.5

4.6.4 Fatigue resistance

The stress levels applied to the mixtures B4 and B5 for the fatigue tests are summarized in Table 37. As shown, higher stress levels compared to the other studied mixtures were applied. This was due to the high stiffness of the materials containing RAP.

Table 37. Stress levels applied for the fatigue tests.

Mixture	σ_0 [MPa]
B4	0.30, 0.40, 0.50, 0.60, 0.70
B5	0.35, 0.40, 0.50, 0.60, 0.70

In Figure 43, the Wohler curves and the initial stiffness of the mixtures are displayed. As shown, the fatigue laws for the two mixtures are almost parallel and very near each other indicating similar behavior in terms of fatigue resistance. However, the mixture without fibres (B4) seems to behave a little bit better than the mixture with fibres (B5).

a)

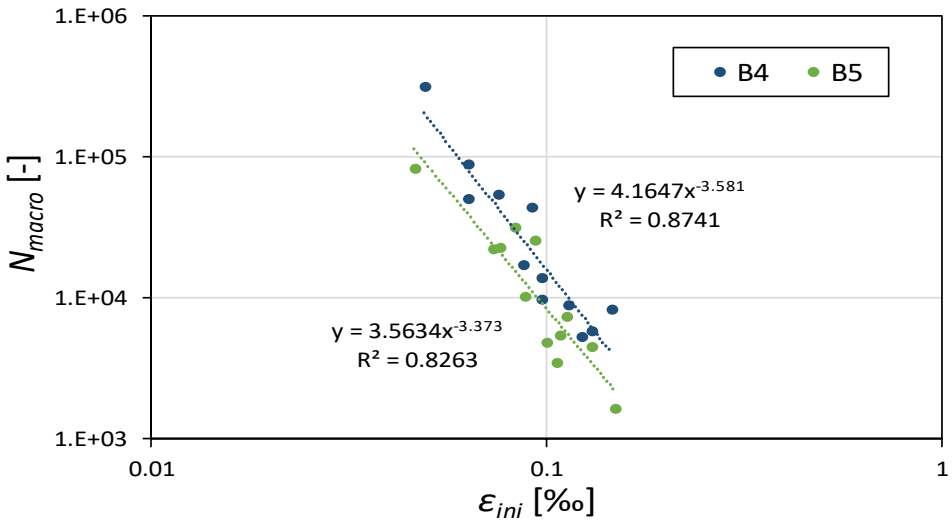

b)

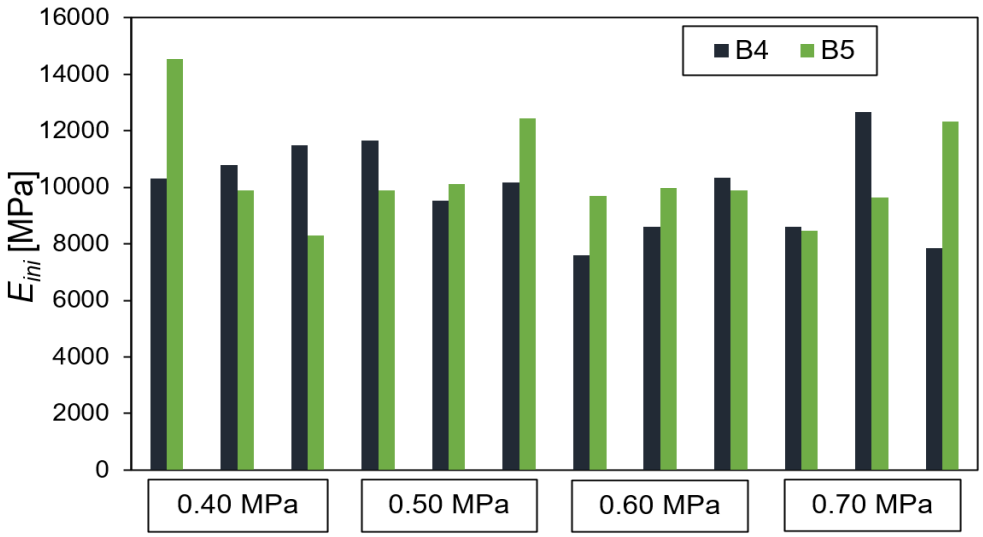

Figure 43. Fatigue results for the mixtures of the binder layer containg RAP at f=10 Hz and at 20°C: a) loading cycles to fatigue failure Nmacro vs initial strain level; b) initial stiffness

4.6.5 Thermal cracking resistance and fracture energy

In Table 38 and Figure 44, the fracture temperatures and the fracture stresses resulting from the TSRST on the mixtures containing RAP are summarized. The failure temperatures are much lower than the values obtained for the binder layer mixtures B1 and B2 reported in Table 17. This is due to the negative stiffening effect at low temperature of the aged RAP binder incorporated to B4 and B5. The difference between the failure temperatures of the two RAP mixtures is almost 7°C. The mixture B4 composed with PmB binder, RAP and without fibres can be applied on cold climate Class II, while the mixture B5 composed with 50/70 binder, RAP and fibres can be used in cold climate class I. Therefore, the FRAM B5 mixture is not able to reach the thermal cracking properties of the reference B4 mixture with PMB.

Table 38. Results of the TSRST.

Mixture	Failure Temperature T_F [°C]	Failure Stress σ_F [MPa]
B4	-23.0	4.371
B5	-16.2	3.039

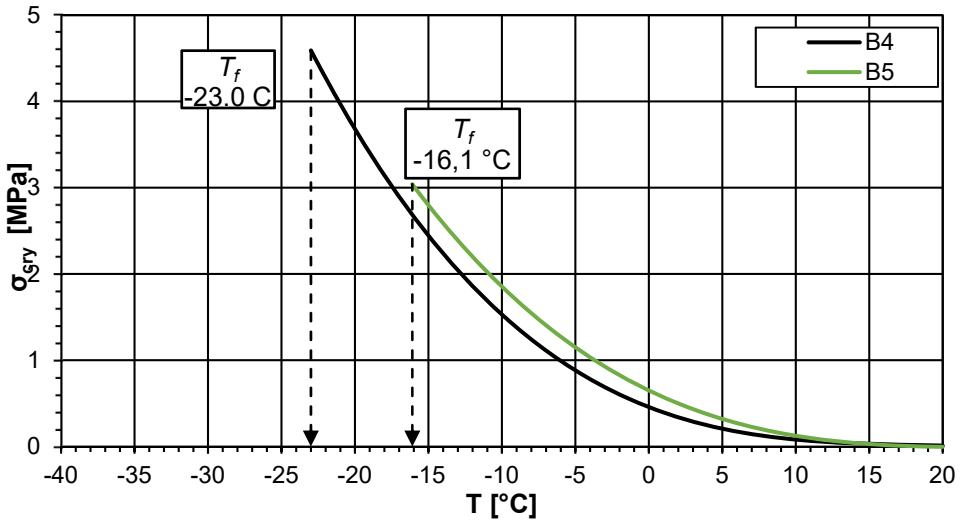

Figure 44. TSRST results: mean cryogenic stress σcry(T) versus temperature for the mixtures of the binder layer mixtures containg RAP.

In Figure 45, the results of the SCB are shown. In particular, the comparison of sigma vs. relative CMOD curves between three different samples of mixture B5 is illustrated. Within these three samples, the values of peak load and slope trend after peak are very similar. Hence, the combined use of RAP and fibre can also lead to homogenous materials.

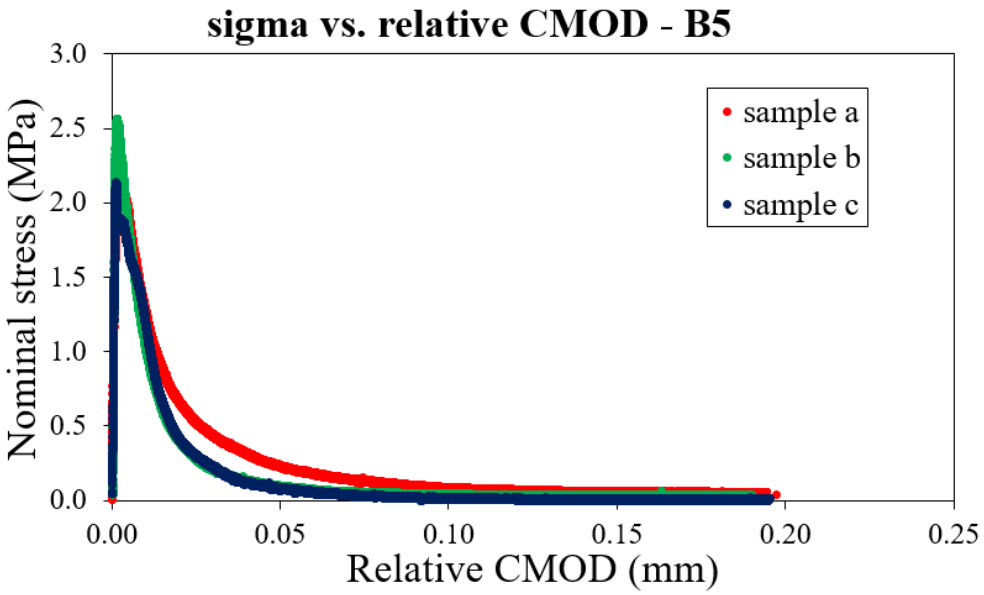

Figure 45. Comparison curves of different samples in B5.

The calculated parameters are listed in Table 39, while the compared curves between B4 and B5 are shown in Figure 46. Comparing the mixtures B4 and B5, only limited differences can

be found in nominal stress, and very similar fracture energy and fracture toughness can be observed. The comparison curves in Figure 46 confirmed this finding. For the binder layer mixtures prepare without RAP, the bitumen type can significantly influence the results; however, this is not true for binder layer mixtures produced with RAP. The use of RAP can mitigate the effect of bitumen type. Hence, when RAP is used to prepare the mixture, unmodified bitumen together with fibre can be an alternative of the PmB bitumen.

Table 39. SCB calculated parameters for binder layer with RAP at -18 °C.

Mixture	σ_{max} [MPa]	G_F [J/m^2]	K_{IC} [MPa*m$^{1/2}$]
B4	3.996	0.557	29.848
B5	3.431	0.585	25.482

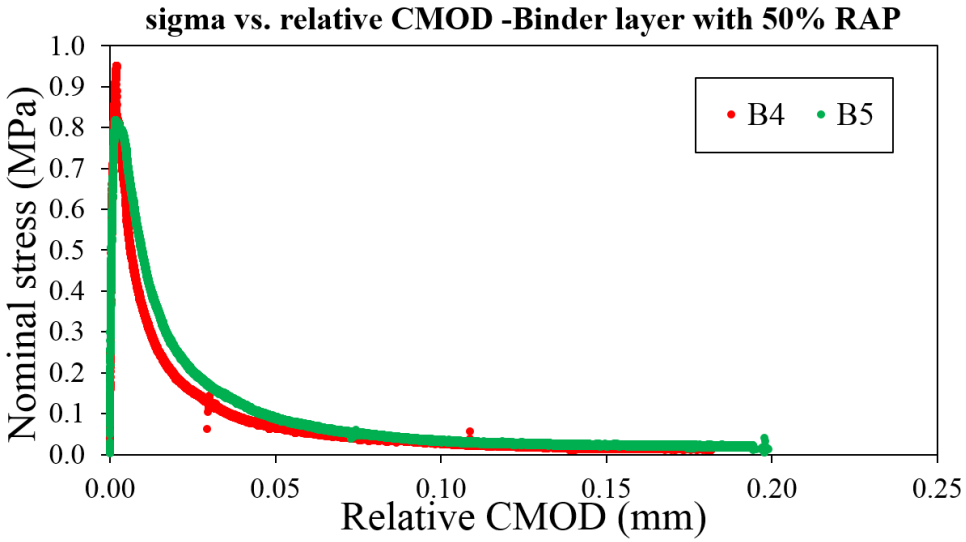

Figure 46. Curve comparison between B4 and B5 for binder layer mixture with RAP

5 Summary and Conclusions

In this deliverable, the performance of fibre-reinforced asphalt mixtures types AC and PA is experimentally investigated.

At the surface layer scale, the set of polyolefin-aramid fibres (Type A) was employed to analyze the reinforcing effect in the PA mix. Five different PA mixtures with and without fibres were prepared for comparison purposes. Air voids, Cantabro test, ITS and moisture sensitivity were the chiefly tests taken into consideration. Concerning the AC mixtures, the 4 mm long polyacrylonitrile fibre (Type P) was the fibre incorporated. Different sets of AC mixtures with and without fibres were manufactured and studied in the different layers of the pavement structure. Besides, the potential recyclability of FRAMs was studied producing artificially aged fibre-reinforced RAP (PANRAP). Finally, the feasibility of incorporating RAP without the presence of rejuvenators in the surface (30%) and binder layer (50%) was investigated. Volumetric properties, ITS, moisture sensitivity, rutting, stiffness, fatigue resistance, thermal cracking and fracture energy were the main tests considered for comparison purposes. In the light of the findings obtained from this extensive experimental study, the following conclusions can be drawn.

PA mixtures at surface layer

- The incorporation of polyolefin-aramid fibres does not affect notably the functional performance of the mixture. The FRPA mixes presented in both cases a porosity greater than 20%.
- FRPA 2 mixture manufactured with polyolefin-aramid mixture showed the highest raveling resistance in dry conditions followed by the mixture manufactured with PMB. Regarding the particle loss in wet conditions, the increase of the binder content is needed to adequately cover the fibres and hence achieved an effective reinforcement of the mixture.
- Mixes manufactured with polyolefin-aramid fibres showed the highest tensile strength in dry conditions as compared to the reference mixtures. In wet conditions, the FRPA 2 mix displayed also the most outstanding value followed by the mix prepared with PMB.
- It is recommended to use high percentages of bitumen in order to ensure the proper coating of the fibres.
- Thermal cracking resistance and fracture energy are worse than the reference mixture with PMB. Therefore, the addition of fibres does not make PA mixtures more suitable for cold regions than PMB.

AC mixtures at surface layer

- All the AC mixtures, including the designs with PANRAP and 30% RAP, showed adequate air voids content in the mixture between the range of 4.00% and 6.00%. Not too many variations were observed in terms of Marshall Stability and flow values among all designs.
- Regarding ITS and moisture sensitivity results, adding fibres increased the tensile

strength in both dry and wet conditions. Besides, mixes prepared with PANRAP, and 30% RAP displayed greater values in tensile strength. The reinforcing effect of fibres was also noticed in these mixtures. In any case, all mixes presented a suitable moisture resistance capability with ITSR values higher than 85%.

- Rutting performance of FRAC was significantly better than AC control. In case of mixtures with PANRAP the behaviour was also improved, but in this case the impact is less evident due to the addition of PANRAP.
- Regarding stiffness test results, adding fibres stiffen slightly the mixture and minimize the phase angle making the mix more elastic. With respect to the addition of fibres to the mixes with PANRAP and real RAP, the dynamic modulus and phase angle were similar than those of the control mixes.
- In relation to fatigue resistance test, it was slightly improved because adding fibres could increase the dynamic modulus while keeping a similar fatigue resistance in comparison to the control AC mixture. On the other hand, a higher percentage of binder could be added without worsen the rutting resistance. Only in the case of the mixture with real RAP, the effect of the fibres was not significant with very similar results between the control and experimental mixtures.
- In general, thermal cracking resistance and fracture energy are not significant modified when fibres are added. The impact of fibres at low temperatures is limited.

AC mixtures at binder and base layers

- For all the AC mixtures for binder (with and without 50% RAP) and base layers, the use of Panacea-aramid fibre lead to a higher tensile strength results in the dry condition. In the case of wet condition, only the binder layer AC mixture without RAP show the same trend. In both binder layer with 50% RAP and base layer mixtures, the materials containing fibres have lower tensile strength values. It indicates that the use of fibre lead to moisture sensitivity materials. Among all the materials, the highest ITS values are observed in the mixture composed with RAP in both dry and wet conditions.
- All the AC mixtures show excellent rutting properties. In the case of binder layer mixtures without RAP, FRAM cannot reach the rutting performance of the polymer-modified mixture. When 50% RAP is used, only limited differences can be found between reference and FRAM. For base layer mixtures, FRAM have better anti-rutting performance than the reference one.
- Regarding stiffness test results, all the FRAM mixtures have similar complex modulus and phase angles with the reference materials. In particular, slightly higher complex modulus and lower phase angle at low frequencies (high temperatures range) can be observed. At high frequency (low temperatures range), slightly low complex modulus and lower phase angle for FRAM are found. Hence, it is to say that similar or even better mechanical properties can be achieved by using fibres.
- For the fatigue properties, in the binder layer mixture without RAP, FRAM gains worse fatigue properties than the reference mixture with the Polymer modified bitumen. This difference is mitigated when RAP is used. In the case of base layer, FRAM mixture has

better fatigue properties even when it uses a harder binder.

- For low temperature properties, all the three FRAM mixtures have worse thermal cracking resistance than the reference materials. In the case of low temperature fracture properties, FRAM mixture is not as good as the reference mixture only in binder layer mixture without RAP. For the other mixtures, both FRAM mixtures and reference mixtures have very similar properties.

From this experimental campaign, it can be concluded that the use of Panacea-aramid fibres in binder and base layers of asphalt pavement together with plain bitumen is unable to reach the comparable properties of the one prepared with high quality PmB bitumen without fibre. In particular, the addition of fibres affects the thermal cracking. Therefore, to implement their use in cold regions, particular attention should be taken. Regarding high temperature performance, the use of fibres leads to improve the resistance against plastic deformation. Regarding fatigue performance, the FRAM show good properties, better than the plain conventional bitumen, without reaching the properties of the high quality PmB.

In case of the porous asphalt, aramid fibres show a good performance strengthening the mixture at dry conditions. They provide a better behaviour than raw bitumen and near to PMB. However, it is required to increase the percentage of bitumen used to improve the performance of PA mixtures at wet conditions, the fibres should be properly coated to avoid the water damage. In this case, the fibres strengthen the samples and increase the anti-draining capacity, so higher percentage of bitumen are available, improving the final performance. These mixtures are still not suitable to be laid in cold regions due thermal cracking has not been improved enough.

The final balance between the environmental and economic impact of the mixtures with fibres respect to the mixtures with PMB seems to be crucial to consider the real possibilities of this technology, due to its mechanical behaviour is between the raw and the modified bitumen in general terms.

Annex A: laboratory protocol

Annex B: Pure Aramid fibre (pulp)

The mixtures developed were designed with the same materials and particle size distribution than FRPA mixtures in order to compare the results. The properties and results of these new aramid fibres were also provided to BAM company.

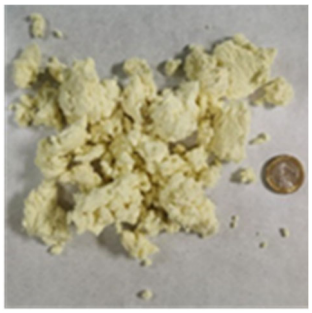

Figure 47. Pure aramid fibres (pulp)

The results of the experimental mixtures with the pure aramid fibre are presented in Table 40. These fibres presented also a good performance, especially against ravelling. Their smaller size seems to make their coating easier. It should be also considered that, in this case, the final quantity of aramid fibre is higher.

Table 40.Mechanical behaviour of PA mixtures reinforced with pure aramid fibres

PA16		**Teijin 1**	**Teijin 2**	**Teijin 3**
Bitumen / mixture (%)		4.5	4.5	5
Type of bitumen		50/70	50/70	50/70
Type of fibre		Aramid	Aramid	Aramid
Fibre / mixture (%)		0.03	0.05	0.05
Voids test (EN 12697 – 8				
Density (g/cm^3)		2.053	2.059	2.070
Voids (%)		21.0	20.7	20.0
Cantabro test in dry (EN 12697 - 17) & wet (NLT 362/92) conditions				
Dry (%)		8.0	5.8	5.1
Wet (%)		11.3	9.2	8.4
Water sensitivity test (EN 12697 – 12)				
I.T.S.	Dry (KPa)	1074.6	990.7	1070.7
	Wet (KPa)	827.3	874.3	805.8
I.T.S.R. (%)		77	88	75
Binder drainage (UNE-EN 12697 – 18)				
Draindown (%)		-	-	0.03